Evaluation of Post-tension Strengthened Steel Girder Bridge Using FRP Bars

CTRE Project 01-99

Sponsored by
the Iowa Department of Transportation
and the Federal Highway Administration

Center for Transportation Research and Education

Bridge Engineering Center

Iowa State University

Final Report • November 2003

CTRE's mission is to develop and implement innovative methods, materials, and technologies for improving transportation efficiency, safety, and reliability while improving the learning environment of students, faculty, and staff in transportation-related fields.

Technical Report Documentation Page

1. Report No.	2. Government Accession No.	3. Recipient's Catalog No.	
4. Title and Subtitle Evaluation of Post-tension Strengthened Steel Girder Bridge Using FRP Bars		**5. Report Date** November 2003 **6. Performing Organization Code** CTRE Project 01-99	
7. Author(s) Terry J. Wipf, Brent M. Phares, F. Wayne Klaiber, and Yoon-Si Lee		**8. Performing Organization Report No.**	
9. Performing Organization Name and Address Center for Transportation Research and Education Iowa State University 2901 South Loop Drive, Suite 3100 Ames, IA 50010-8634		**10. Work Unit No. (TRAIS)** **11. Contract or Grant No.**	
12. Sponsoring Organization Name and Address Iowa Department of Transportation 800 Lincoln Way Ames, IA 50010		**13. Type of Report and Period Covered** Final Report **14. Sponsoring Agency Code**	
15. Supplementary Notes This project was also sponsored by the Federal Highway Administration. This report is available in color at www.ctre.iastate.edu.			

16. Abstract

Many state, county, and local agencies are faced with deteriorating bridge infrastructure composed of a large percentage of relatively short to medium span bridges. In many cases, these older structures are rolled or welded longitudinal steel stringers acting compositely with a reinforced concrete deck. Most of these bridges, although still in service, need some level of strengthening due to increases in legal live loads or loss of capacity due to deterioration. Although these bridges are overstressed in most instances, they do not warrant replacement; thus, structurally efficient but cost-effective means of strengthening needs to be employed. In the past, the use of bolted steel cover plates or angles was a common retrofit option for strengthening such bridges. However, the time and labor involved to attach such a strengthening system can sometimes be prohibitive.

This project was funded through the Federal Highway Administration's Innovative Bridge Research and Construction program. The goal is to retrofit an existing structurally deficient, three-span continuous steel stringer bridge using an innovative technique that involves the application of post-tensioning forces; the post-tensioning forces were applied using fiber reinforced polymer post-tensioning bars. When compared to other strengthening methods, the use of carbon fiber reinforced polymer composite materials is very appealing in that they are highly resistant to corrosion, have a low weight, and have a high tensile strength.

Before the post-tensioning system was installed, a diagnostic load test was conducted on the subject bridge to establish a baseline behavior of the unstrengthened bridge. During the process of installing the post-tensioning hardware and stressing the system, both the bridge and the post-tensioning system were monitored. The installation of the hardware was followed by a follow-up diagnostic load test to assess the effectiveness of the post-tensioning strengthening system. Additional load tests were performed over a period of two years to identify any changes in the strengthening system with time. Laboratory testing of several typical carbon fiber reinforced polymer bar specimens was also conducted to more thoroughly understand their behavior. This report documents the design, installation, and field testing of the strengthening system and bridge.

17. Key Words	18. Distribution Statement		
bridge infrastructure deterioration—bridge load testing—fiber reinforced polymers—post-tensioning forces	No restrictions.		
19. Security Classification (of this report)	**20. Security Classification (of this page)**	**21. No. of Pages**	**22. Price**
Unclassified.	Unclassified.	71	NA

EVALUATION OF POST-TENSION STRENGTHENED STEEL GIRDER BRIDGE USING FRP BARS

CTRE Project 01-99

Co-Principal Investigators
Terry J. Wipf, P.E.
Professor of Civil Engineering, Iowa State University
Manager of Bridge Engineering Center
Center for Transportation Research and Education

Brent M. Phares, P.E.
Associate Director for Bridges and Structures
Center for Transportation Research and Education

Investigator
F. Wayne Klaiber, P.E.
Professor of Civil Engineering, Iowa State University

Research Assistant
Yoon-Si Lee
Graduate Student
Bridge Engineering Center, Iowa State University

Preparation of this report was financed in part
through funds provided by the Iowa Department of Transportation
through its research management agreement with the
Center for Transportation Research and Education.

Also sponsored by the Federal Highway Administration

Center for Transportation Research and Education
Iowa State University
2901 South Loop Drive, Suite 3100
Ames, IA 50010-8634
Phone: 515-294-8103
Fax: 515-294-0467
www.ctre.iastate.edu

Final Report • November 2003

TABLE OF CONTENTS

LIST OF FIGURES

LIST OF TABLES

ACKNOWLEDGMENTS

The authors would like to thank the Iowa Division of the Federal Highway Administration for their support on this project and extend their sincere appreciation to the numerous Iowa Department of Transportation personnel, including those with the Offices of Bridges and Structures and Maintenance who provided significant assistance with the field testing. Special thanks are extended to Curtis Monk (Federal Highway Administration–Iowa Division bridge engineer), Ahmad Abu-Hawash (Iowa Department of Transportation chief structural engineer), and Norman McDonald (Iowa Department of Transportation bridge engineer) for their help in various phases of the project. Bridge engineers Frank Russo and Tom Sardo (who have since left the Iowa Department of Transportation) are also thanked for their contributions. Special thanks are also accorded to Douglas L. Wood (Iowa State University Structural Engineering Laboratory manager) for his assistance with the system installation and the laboratory and field testing.

1. INTRODUCTION

1.1. Background

Based on data from the Federal Highway Administration (FHWA), approximately 30% of the nearly 600,000 bridges in the U.S. are in need of repair or replacement due to structural deficiencies or functional obsolescence. As these bridges continue to deteriorate, the problems have become further compounded by increases in legal load limits. In many cases, strengthening, rather than replacement, is a more cost effective management decision. Yet, common methods for strengthening existing bridges, such as using bolted or welded steel cover plates or angles, are sometimes prohibitive due to the time and labor involved in installing such a retrofit system. Thus, structurally efficient yet cost-effective strengthening methods need to be developed.

In the last decade, the use of fiber-reinforced polymers (FRP) has emerged as a promising technology in structural engineering. This report documents a method of strengthening a structurally deficient bridge through the application of carbon fiber reinforced polymers (CFRP) post-tensioning bars. Among the various strengthening materials, the use of CFRPs is very appealing in that the CFRPs are highly resistant to corrosion, have a low weight, and have a high tensile strength.

The bridge selected for strengthening was a three-span continuous rolled shape bridge in Guthrie County, Iowa, on state highway IA 141 approximately 1.6 miles west of Bayard, Iowa. The goal of this project was to design and install the CFRP post-tensioning bars on the steel girders and to monitor and document the performance and long-term impact of the strengthening system.

1.2. Literature Review

1.2.1. Post-tensioning

The general purpose of using external post-tensioning (P-T) on an existing bridge is to restore its load carrying capacity by applying internal loads that counteract the dead and live load stresses. External P-T can be very economical, adaptable, and effective in that bars can be easily inspected and, if necessary, be replaced. This makes P-T a viable alternative for strengthening existing structures since installation of the strengthening system is independent of other maintenance operations. The major drawback associated with the use of external P-T is exposure of the hardware to both environment conditions and potential impact.

Since the early 1980s, the Iowa Department of Transportation (Iowa DOT) has developed the concept of strengthening simple-span and continuous-span bridges by P-T through several research projects. Klaiber et al. [1] and Dunker et al. [2, 3, 4] completed several projects related to the use of external P-T with high strength steel bars for the purpose of upgrading the live-load carrying ability of steel beam, composite concrete deck bridges. This collection of work includes both experimental and analytical results to demonstrate the effectiveness of external P-T. The initial project, entitled “Feasibility Study of Strengthening Existing Single Span Steel Beam Concrete Deck Bridges” [1] and published in June 1981, studied the general concepts of strengthening single-span bridges by P-T. To illustrate these concepts, a 1/2-scale simple-span,

steel-girder, concrete slab bridge was tested in the laboratory with numerous P-T schemes. The most promising concepts were later tested and demonstrated in the project "Strengthening of Existing Single-Span Steel-Beam and Concrete Deck Bridges" [3]. The general objective of this work was to design and install post-tension strengthening systems on two existing simple span bridges in Iowa. As a follow-up, a document, *Design Manual for Strengthening Single-Span Composite Bridges by P-T* [4], was developed for use by design engineers. Based on the successful implementation on single-span composite bridges, further work was completed to examine the feasibility of strengthening continuous-span bridges using P-T [5]. A design recommendation for the strengthening of continuous-span bridges was then developed by Klaiber et al. [6]. The methodology employed was to utilize the P-T technique in the positive moment regions and superimposed trusses in the negative moment regions. A methodology for determining required amount of P-T force and retrofit scheme (location of P-T system) to reduce or eliminate overstresses in bridges of various configurations was presented in the final report. The results of these research projects verified that the P-T system could effectively be used on continuous-span bridges. Although the P-T system did not significantly reduce live load deflections, it did slightly increase the load carrying capacity of the bridge, thus allowing the bridges to carry additional live loads.

The proven methodology presented in these reports has been successfully used on single-span as well as continuous bridges by engineers in the Iowa DOT and other agencies to improve or upgrade the condition of those bridges such that they meet the demands of modern transportation standards. This collection of work was the basis for the system described in this report.

1.2.2. Carbon Fiber Reinforced Polymer

CFRP materials have been predominantly used by the aerospace industry where cost is generally a secondary consideration to weight [7]. Although the initial cost is typically higher than other conventional materials, CFRP is high in strength and modulus, low in density, chemically resistant, and has outstanding thermal and electrical conductivity properties.

Carbon fibers were first used in a civil application at the Swiss Federal Testing Laboratories [8]. Although it was viewed as generally uneconomical due to the material cost, it was found to be more effective when the reduced on-site construction time was considered.

Since 1975 when the first pedestrian FRP bridge was built by the Israelis, FRP materials have been used in the construction of pedestrian bridges in many continents [9]. Based on the knowledge and experience obtained from working with pedestrian bridges, many engineers, scientists, and researchers have attempted to extend the applicability of FRP to vehicular bridges. Since the early 1990s, many bridge deck systems have been developed and tested utilizing this innovative material. In addition, structural shapes have been developed and tested for use in replacing deteriorated superstructure elements. However, it has typically been found that the most economical use of FRP occurs when it is used with conventional bridge materials.

1.3. Objectives

The primary objective of the project was to investigate and evaluate the effectiveness of CFRP bars to strengthen an existing, structurally deficient, steel girder bridge. Secondary objectives of this project were as follows:

- Document the construction and performance of the innovative material used.
- Monitor the behavior of the bridge during the application of the P-T.
- Identify changes in structural behavior due to the addition of the strengthening system and with time through field inspection and periodic load tests.

1.4. Scope

The research program consisted of several tasks with the main emphasis being the installation of the strengthening system and associated field testing. Before the P-T system was installed, a diagnostic load test was conducted on the subject bridge to establish a baseline behavior of the unstrengthened bridge. During the process of installing the P-T hardware and stressing the system, both the bridge and the P-T system were monitored. The installation of the hardware was followed by a follow-up diagnostic load test to assess the immediate effectiveness of the P-T strengthening system. Additional load tests were performed over a two-year period to identify any changes in the strengthening system with time. After the last follow-up test (two years of service) was completed, the P-T force was removed from the bridge (and re-applied) to investigate any losses that may have occurred over the two-year period. Laboratory testing of several typical CFRP bar specimens was also conducted to more thoroughly understand their behavior.

A detailed description of the subject bridge and the strengthening system employed is given in Chapter 2. The various tests conducted in the laboratory and in the field are described in Chapter 3, and the corresponding test results are summarized in Chapter 4. Following the test results, the summary and conclusions are presented in Chapter 5.

2. BRIDGE AND STRENGTHENING SYSTEM DESCRIPTION

This chapter describes the physical characteristics of the strengthened bridge. Also, a description of the strengthening system and its installation is given.

2.1. Bridge Description

The bridge (Number 3903.0S 141) selected for strengthening is a 210 ft x 26 ft, three-span continuous, rolled shape steel girder bridge constructed in 1956 (shown in Figure 1). It is located in southwest-central Iowa in Guthrie County approximately 1.6 miles west of Bayard, Iowa, carrying state highway IA 141 over Willow creek. The bridge consists of two 64-ft end spans and a 82-ft center span. Bridge beams are spliced at locations 20 ft from the two piers in all spans (i.e., four splices per beam line). The bridge deck is a nominal 7-in. thick cast-in-place, reinforced concrete slab that was overlaid with dense low-slump portland cement concrete (PCC) in 1987. The current average deck thickness is approximately 10 in., including 3 in. of wearing surface with 2 1/2 in. of crown. The bridge deck is supported by two WF 30x116 exterior and two WF 33 1/4x141 interior I-beams spaced at 8 ft-3 in. on center as shown in Figure 2. The abutments are stub reinforced concrete and the piers consist of open-two-concrete columns with cantilevers. Abutments and piers are both supported on steel piling. The abutments have sliding steel plate bearings while the piers have rocker-type bearings. The roadway width is 26 ft allowing two traffic lanes with one lane in each direction and a narrow shoulder on each side. The bridge has moderate curbs that are integral with the deck and concrete guardrails connected to the curbs.

Both abutments show a few hairline cracks. Severe corrosion was found at the abutment bearings and moderate to severe spalls were found near the back wall and the bottom of the concrete deck (see Figure 1d). There are signs of moderate to severe corrosion on the exterior beams, and areas with moderate to severe corrosion on the bottom flanges of the abutment diaphragms. Also, a considerable amount of corrosion is present on the deck channels and the top of the web of the curb channels (see Figure 1e). The bridge deck has several hairline and narrow transverse cracks. Both curbs show moderate hairline cracks and small spalls at several locations.

2.2. Strengthening System

The P-T based strengthening system utilized was developed based on the strengthening recommendations of Klaiber et al. [6] and material performance data provided by the manufacturer. CFRP bars were selected due to their outstanding mechanical characteristics and non-corrosive nature. The installation of the P-T system was completed in the positive moment region of the exterior girders in all three spans. The bridge has welded cover plates in the negative moment regions which were determined to be adequate and, therefore, not in need of strengthening. A total of 12 kips was applied to each bar (four bars per location). The descriptions of the design process, the strengthening system components, and the installation procedures are presented in the following sections.

(a) Side view

(b) End view

Figure 1. Overall bridge photographs.

(c) Bottom view

(d) Typical east abutment condition

Figure 1. Overall bridge photographs (continued).

(e) Typical condition of deck soffit and deck channel

Figure 1. Overall bridge photographs (continued).

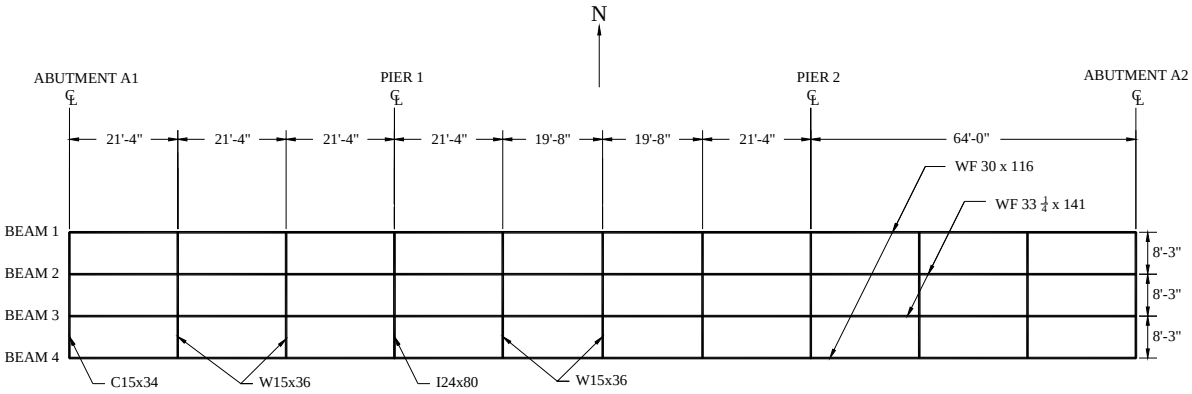

Figure 2. Bridge framing plan.

2.2.1. Design Process of Post-tensioning Strengthening System

The design of the CFRP P-T strengthening system was completed for the HS-20 load [10] using the allowable stress design (ASD) approach. Based on analysis completed by the bridge owner, it was found that the positive moment region of the exterior beams (Beam 1 and Beam 4) in both

the end and center spans was overstressed. This section describes the several steps followed in designing the P-T strengthening system. Although some hand calculations were required, a spreadsheet was used for a majority of the computations needed to determine the required P-T force at each location. A description of detailed design methodologies and use of the design spreadsheet is presented in Reference 6. The steps to determine the required P-T forces are summarized as follows:

1. Section properties of all girders are computed.
2. All loads and load fractions for each beam are computed for dead load, long-term dead load, and live load plus impact.
3. Internal moments and resulting stresses in each girder induced by the loads computed in Step 2 are determined at various sections along the length of the bridge.
4. The strengthening scheme, bar lengths, and location are selected.
5. Overstresses that need to be reduced are computed.
6. The P-T forces that would generate the desired stress reduction at the critical sections are determined.
7. The final stresses in all girders are checked to ensure that stresses are within the allowable stress limit.
8. The P-T strengthening forces are increased by 8% to account for time-dependent losses and errors due to approximations in the design methodology [6].
9. With the increased P-T force, the stress check procedure (Step 7) is repeated.

2.2.2. CFRP Post-tensioning Strengthening System Components

The CFRP bar used in this project is 3/8 in. in diameter and has a high tensile strength, a moderate modulus of elasticity, low creep properties, and a high resistance to corrosion. For connection to the other P-T system components, the CFRP bar is embedded into steel tube anchors that have threaded ends. Material properties of the CFRP bars are listed in Table 1.

Table 1. Material properties of CFRP bar.

Diameter (in.)	Tensile strength (ksi)	Tensile modulus (ksi)	Elongation at ultimate	Fiber content
3/8	300	20,000	1.5%	65% by volume

The CFRP bars were connected to the steel beams with 5 in. x 5 in. x 3/4 in. stiffened angles 7 in. in length. Each of these stiffened angle assemblies, which are connected to the web of the steel beams with two 1 in. diameter, and 3 1/2 in. long A325 high-strength bolts, connects four CFRP bars to the web of the beam (two on each side) near the bottom flange. The details of the anchorage assemblies are illustrated in Figures 3 and 4.

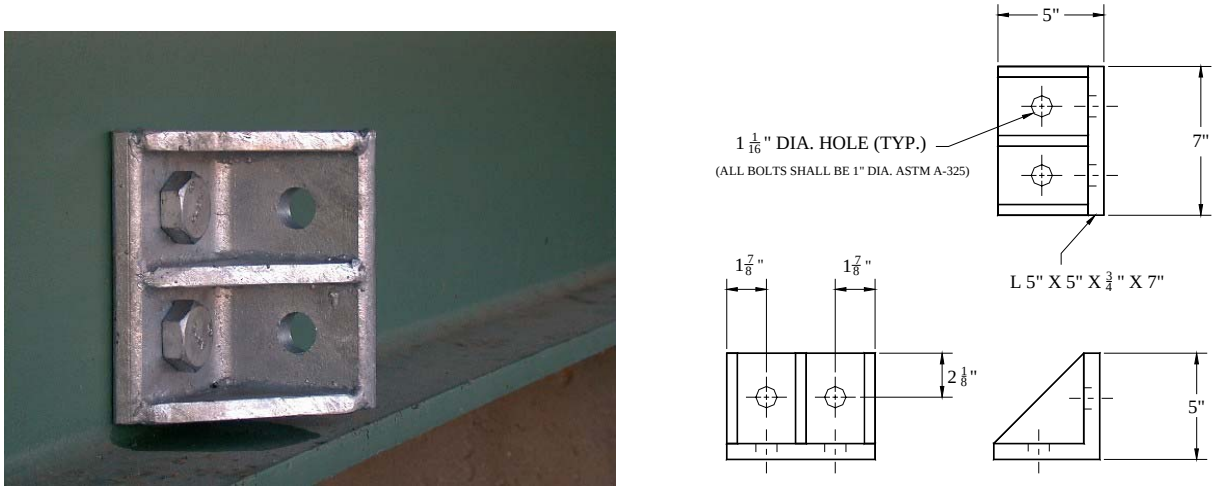

(a) Stiffened steel angle assembly

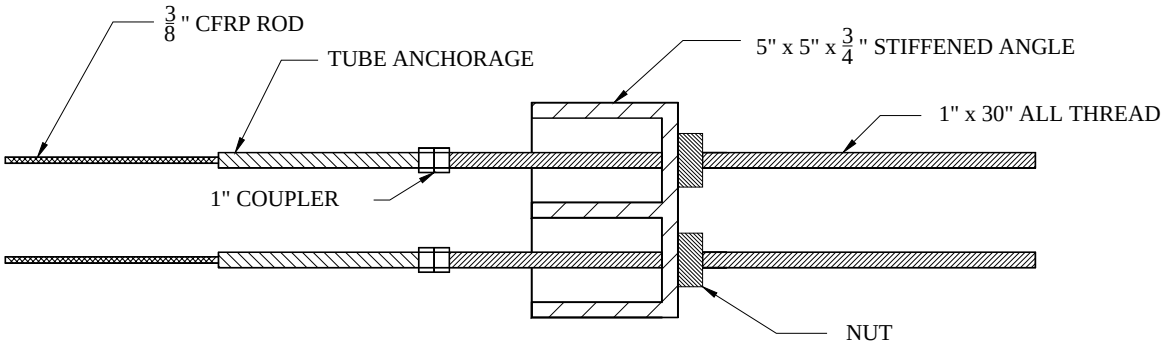

JACKING END

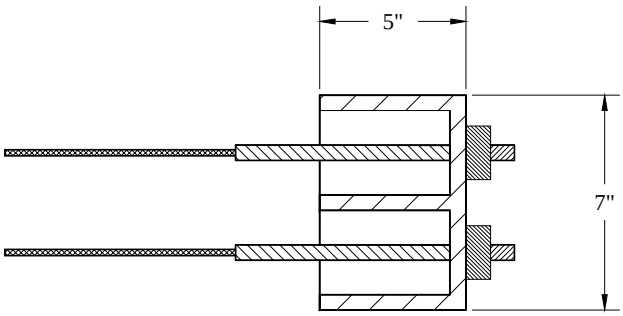

FIXED END

(b) CFRP bar to bracket connection detail

Figure 3. Anchorage assembly detail for P-T bars.

2.2.3. Installation Procedure of CFRP Post-tensioning Bars

As previously stated, the P-T system was installed in the positive moment region of the exterior girders in all three spans of the bridge. Installation of the complete system was completed in just one day by a three-man crew with no special training required. Given accessibility limitations, some of the installation procedures were completed from a man-lift located below the bridge. The following lists and briefly describes the principal installation steps:

1. The location of the anchorage assemblies shown in Figure 4 were determined based upon the original design and field measurements.
2. 1 1/16 in. diameter holes were drilled through the web of each exterior beam for attaching the stiffened angle anchorage assemblies.
3. The surface of the web that was to be in contact with each stiffened angle anchorage assembly was cleaned without paint removal. All other foreign materials, such as burrs and metal shavings due to drilling of holes, were removed to allow for a satisfactory surface contact for a bolted friction connection.
4. The anchorage assemblies were then bolted to the webs of the beams with 1 in. diameter A325 high-strength bolts torqued in accordance with the manufacturer's recommendation (Figure 5).
5. As shown in Figure 6, interference between the CFRP bars and the diaphragms was corrected by removal of a portion of the diaphragm/stiffener assembly with an acetylene torch.
6. The CFRP P-T bars were placed in position between anchorage assemblies on both sides of the web (Figure 7). Extra caution was taken during the erection not to damage any of the bars by scratching or excessive sagging.
7. A nominal force of 12 kips was applied to all bars (four bars per location) with a hollow-core hydraulic jack in a symmetrical manner following the sequence of steps listed below and illustrated in Figure 8, where each event defines a specific step in the P-T process:
    a. A nominal force of 6 kips was applied to the bottom and then to the top bar on the south side of the south exterior girder (Beam 4) in the west end span (Events 1–4).
    b. A nominal force of 6 kips was applied to the bottom and then the top bar on the north side of the south exterior girder (Beam 4) in the west end span (Events 5–8).
    c. Steps 1 and 2 were repeated in reverse order to increase the nominal force of 6 kips in each bar to the intended force of 12 kips (Events 9–16), thus completed the P-T at one location.
    d. The jacking equipment was then moved to the north exterior girder (Beam 1) and Steps a through c were repeated (Events 17–32) for the four bars at that location.
    e. Steps a through d were then repeated in the center span (Events 33–64) and in the east end span (Events 65–96) to complete the P-T.

A complete list of "Events" occurring during the application of the P-T force is presented in the Appendix. Photographs of the application of P-T force in the west end span and center span are shown in Figure 9, and the overall construction sequence is illustrated in Figure 10. Also, photographs of the completed installation can be seen in Figure 11.

Generally, the handling and installation process of the CFRP P-T system was relatively simple

and not labor intensive requiring less than five man-days to install. It is recommended, however, that a visual inspection be made at each rod grip after the force is applied to the system to make sure that no slippage has occurred between the bars and the grips.

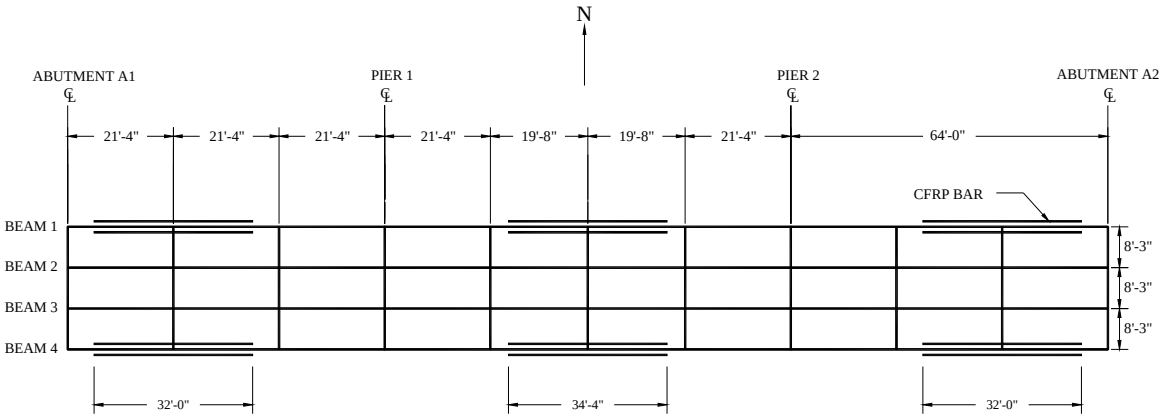

(a) Plan view

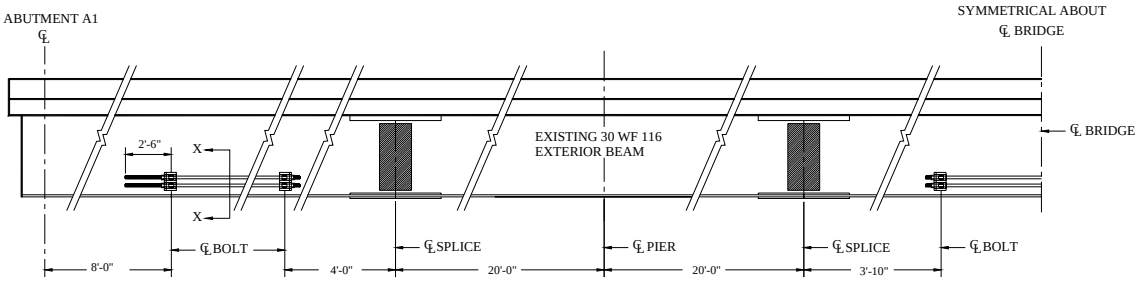

(b) Side view

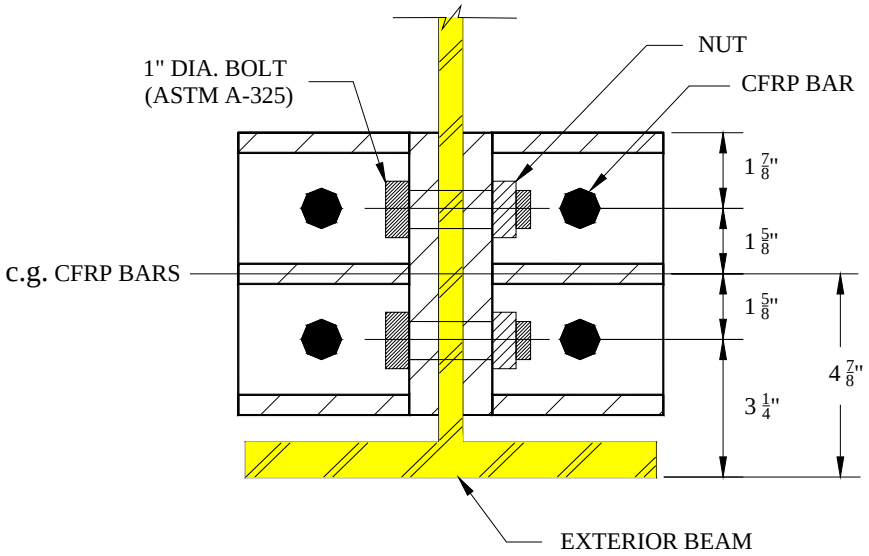

(c) Section X-X

Figure 4. Location of the P-T system on the bridge.

Figure 5. Installing anchorage assembly.

Figure 6. Removal of a portion of the diaphragm/stiffener assembly.

(a) Placement of a CFRP bar

(b) Top CFRP bar in place

Figure 7. Installation of CFRP bars.

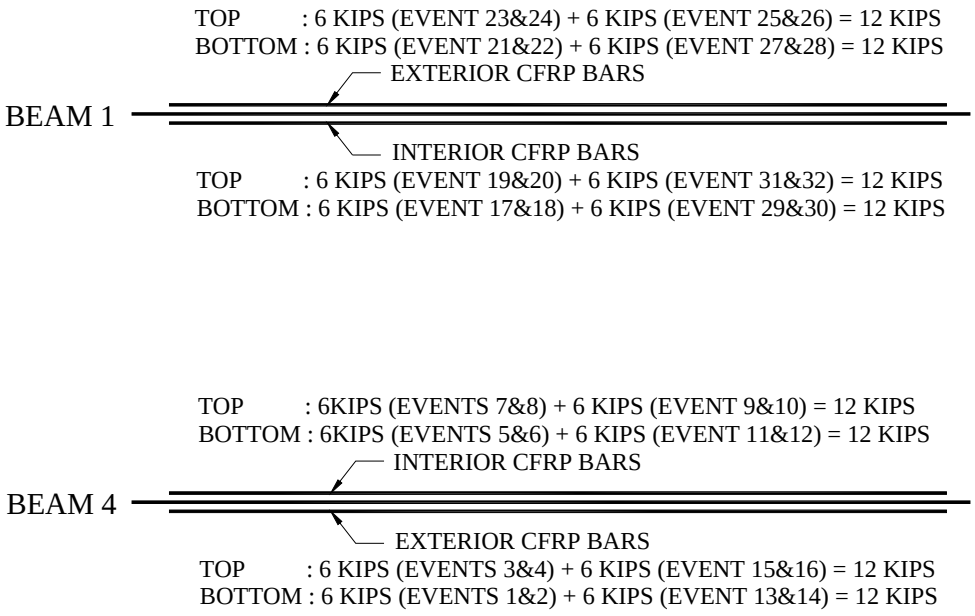

Figure 8. Typical P-T application sequence.

(a) Application of P-T force in the west end span

(b) Application of P-T force in the center span

Figure 9. Application of P-T force.

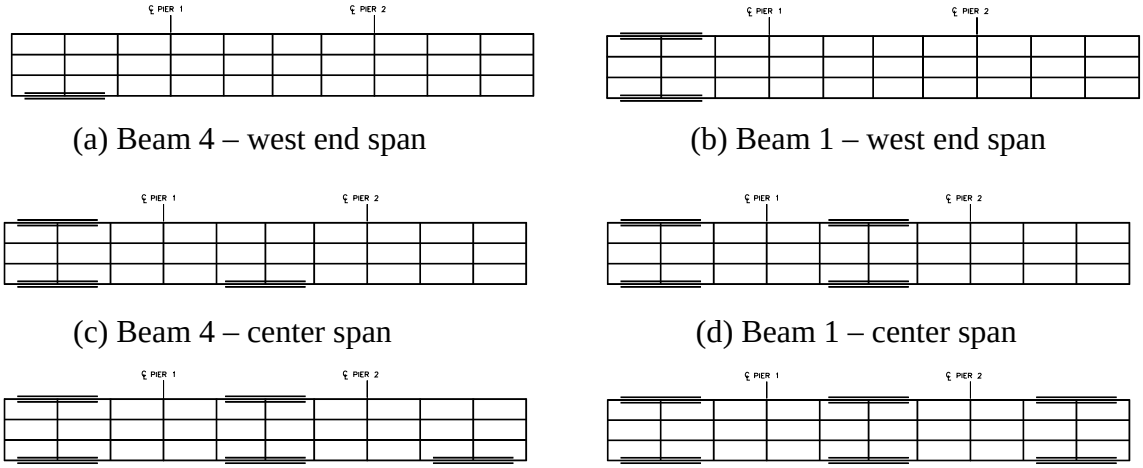

(a) Beam 4 – west end span

(b) Beam 1 – west end span

(c) Beam 4 – center span

(d) Beam 1 – center span

(e) Beam 4 – east end span

(f) Beam 1 – east end span

Figure 10. Overall P-T sequence.

(a) Exterior CFRP bars in west end span

Figure 11. Photographs of the completed installation.

(b) Interior CFRP bars in west end span

(c) CFRP bars in center span

Figure 11. Photographs of the completed installation (continued).

3. EXPERIMENTAL PROGRAM

This chapter describes the various tests conducted in the laboratory and in the field to evaluate the performance of the CFRP P-T strengthening system. Twenty-four hour, constant load and ultimate tensile strength tests were conducted in the laboratory to evaluate important material characteristics. The bridge described previously was instrumented to measure flexural strains at strategically selected locations; it was tested before installation of the P-T strengthening system, immediately following installation, and after approximately one and two years of service to assess changes in the live load response resulting from the addition of the P-T strengthening system and time. In addition, the behavior of the bridge was monitored during the application of P-T forces. The following sections describe each test performed with the results of the testing and evaluation presented in Chapter 4.

3.1. Laboratory Testing

The creep and tensile behavior for conventional materials such as steel are well known; however, these characteristics are not well established for composite materials such as CFRP bars. Laboratory tests were performed to help define the characteristics and to further investigate the feasibility of using this material in P-T strengthening systems. Originally, the laboratory testing program was to include only ultimate strength testing of a sample of CFRP bars. However, within 24 hours of installation of the CFRP bars on the subject bridge, slip was observed to have occurred at the bar to steel tube anchor interface (see Figure 12). Although a large slip (approximately 1 in.) occurred at one of the CFRP bars (bottom bar on the west end span Beam 4), most locations had relatively small amount of slip (i.e., in the range of 1/16 in. to 1/8 in.). To this end, the laboratory testing program was modified to include loading sample bars under constant force to study the slippage phenomenon. The following paragraphs describe the specimens tested and the two types of tests performed.

The CFRP bar specimens tested in the laboratory, shown in Figure 13, had a total length of 54 in. with the same 3/8 in. diameter and other properties as the CFRP bars used in the field P-T strengthening system. Both ends of the CFRP bar were embedded in 12 in. long steel tube anchorage, as was used in the field.

A total of eight CFRP bars (designated from S1 through S8) were examined. The 24-hour, constant load tests were conducted on three bars (S1, S2, and S3). Ultimate strength tests were conducted on eight bars (S1 through S8), including the three bars that were initially tested under constant load for 24 hours.

The ultimate strength and 24-hour, constant load tests were performed on the eight specimens to examine grip performance, to gain a better understanding of their basic engineering properties, and to study the general suitability as a strengthening material. Both tests required similar setups. All tests were completed using a Satec 400HVL test machine with 400 kips capacity and a 12 in.-stroke in conjunction with an Optim Megadac data acquisition system Model 3415AC. Two Direct Current Displacement Transducers (DCDT) gages were installed on each specimen close to the grips to measure the slip between the bar and tube anchorage (see Figure 14).

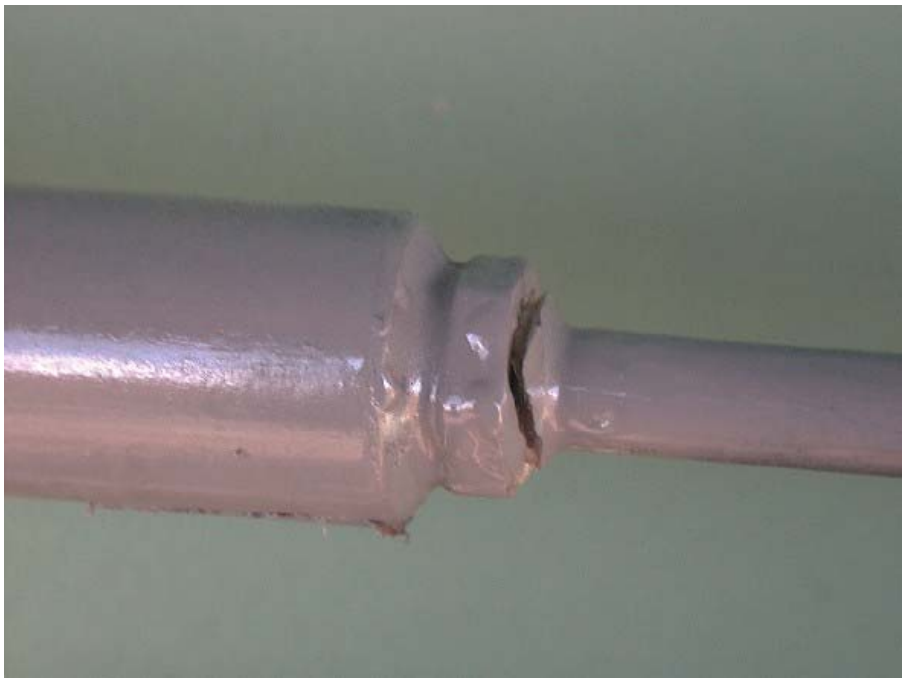

Figure 12. Slip between the CFRP bar and the steel tube anchor interface.

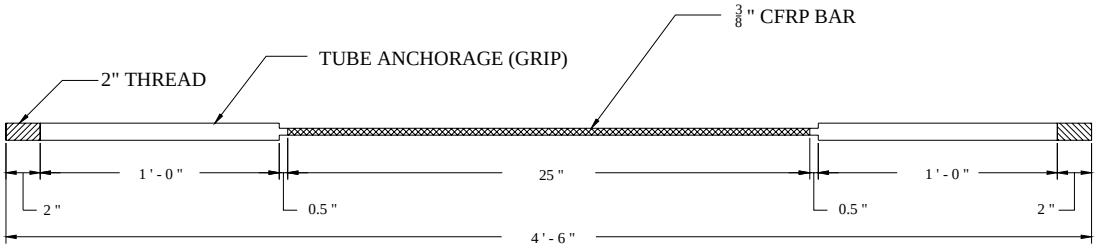

(a) Configuration of CFRP bar specimen

(b) Photograph of CFRP bar

Figure 13. CFRP laboratory specimen.

For the 24-hour, constant load test, an electronic extensometer with a 2-in. gage length was mounted at approximately mid-length of the specimens to measure internal strain. Each specimen was installed in the test machine with a connection detail that simulates the connection used in the field P-T strengthening system. Each specimen was installed across the two cross heads of the test machine so that they were aligned with the center of the grips. The top and bottom of the grip ends that had threaded ends were bolted to the top and bottom test machine heads. An example of a fully instrumented specimen and test setup is illustrated in Figure 15.

The primary goal of the 24-hour, constant tests was to observe if there were any significant elongation or separation between the bar and the grip connection during the 24 hours after the force was applied. To this end, each specimen was placed under a constant load of 12 kips for 24 hours to simulate the field conditions. The applied load and elongation were recorded continuously for the duration of the test.

The ultimate tensile strength tests were conducted to determine the ultimate capacity of the CFRP bars. Eight specimens were tested under stroke control until failure. Different loading rates were used to study the impact on the performance of the material. The loading rates used were 5% on specimens S6 and S7, 12% on specimens S1, S3, S4, and S5, and 15% on specimens S2 and S8.

3.2. Field Load Testing

The location of the instrumentation was selected so that the live-load response of the bridge could be determined, thus providing an overall understanding of global behavior. A total of thirty-six strain gages were installed on the bridge with thirty-two gages on the top and bottom flanges of the beams and four gages on the guardrails as illustrated in Figure 16. Due to the structural symmetry of the bridge, only one-half of the bridge was instrumented.

After installation of the instrumentation, a loaded 3-axle dump truck was driven, at crawl speed, across the bridge with strain data collected continuously as the truck crossed the bridge. The initial test was conducted to establish a benchmark response of the bridge, while the follow-up tests were completed to access changes resulting from the addition of the P-T system and time.

3.2.1. Initial Test (October 29, 2001)

A diagnostic initial load test was conducted prior to the installation of the P-T system to establish a baseline static behavior of the unstrengthened bridge. Four different load paths were used to examine the performance of the bridge. For convenience, each load path is referred to as Y1, Y2, Y3, and Y4, respectively, as shown in Figure 17. For path Y1, heading east, the driver side wheel was placed 3 ft north of the bridge centerline. For path Y3, the passenger side wheel was placed on the same path as Y1, but heading west. For path Y2, heading east in north lane, and path Y4, heading west in south lane, the driver side wheels were placed 2 ft from the north and south curbs, respectively. The Iowa DOT provided the loaded truck shown in Figure 18. Truck 1, the truck utilized during the initial test, had a total weight of 55.92 kips with 16.40 kips and 39.52 kips on the front and rear axles, respectively.

3.2.2. Monitoring During Application of Post-tensiong Force

During application of forces to the P-T strengthening system, the bridge and selected CFRP bars were monitored. The goal of this monitoring was to confirm that the design methodology used to predict the distribution of P-T force throughout the bridge was accurate. As illustrated in Figure 19, a calibrated system of strain gages was installed on four CFRP bars (Bar 1, Bar 2, Bar 3, and Bar 4) on Beam 4 in the west end span. In addition, the same instrumentation used during the previously described test was again monitored during application of the P-T forces.

3.2.3. Immediately After Installation (November 9, 2001)

The second load test was conducted shortly following installation of the P-T system to assess any immediate change in performance resulting from the installation of P-T system. The protocols used for the second load test were the same (e.g., same load paths and sequences, location of the strain gages, etc.) as what was used in the initial test except for the weight of the truck used. The load truck used for the second load test, Truck 2, was again provided by the Iowa DOT and had a total weight of 52.16 kips with 14.74 kips and 37.42 kips on the front and rear axles, respectively.

3.2.4. One Year of Service (October 30, 2002)

On October 30, 2002, another follow-up load test was conducted to investigate any change in the behavior of the bridge over a one year time period. The total weight of the test truck used in this test, Truck 3, was 49.20 kips with 12.52 kips on the front axle and 36.68 kips on the rear axle weight. As before, the same testing protocols were followed.

3.2.5. Two Years of Service (June 11, 2003)

On June 11, 2003, the final test was conducted to assess any change in performance over the two-year life of the P-T system. The bridge was instrumented in the same manner as in previous tests and the same truck paths were used. The truck utilized for this test, Truck 4, had a total weight of 45.58 kips with 13.20 kips in the front axle and 32.28 kips in the rear axle. Dimensions and weights of the load truck used in each test are illustrated in Figure 20 and summarized in Table 2.

After the “two years of service” test was completed, the P-T force was removed from the bridge so that any losses that occurred during the two-year period could be determined. Illustrated in Figure 21 is the order in which the P-T forces were removed from the bridge. Corresponding results are documented in Chapter 4. Note that the P-T force on the top bar on Beam 1 in the west end span was not removed due to the short length of the threaded bar at jacking end (too short to set up the hydraulic jack). After determination of the force remaining in each bar, a nominal force of 12 kips was re-applied to each bar (July 9, 2003).

(a) Photograph of instrumented specimen

(b) Top grip

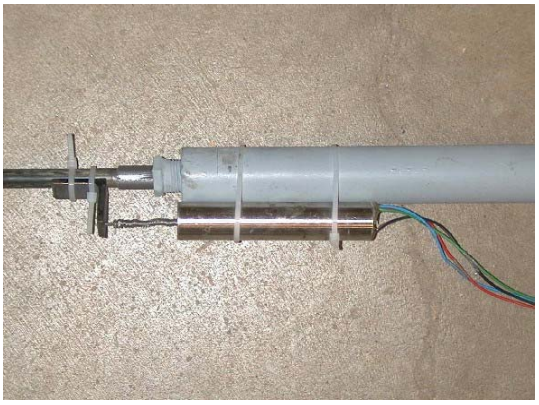

(c) Bottom grip

Figure 14. Slip measurement instrumentation for the laboratory specimen.

Figure 15. Test setup for laboratory testing.

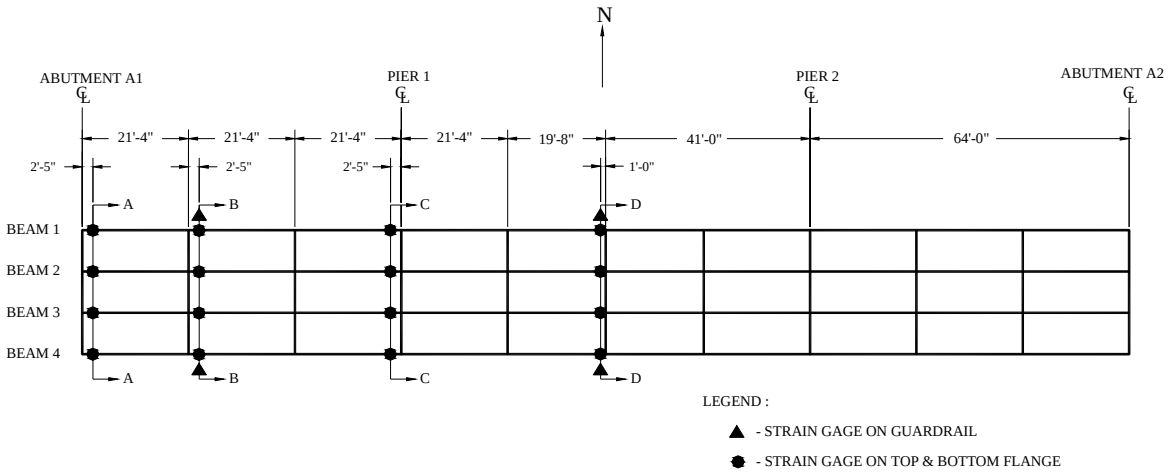

(a) Plan view

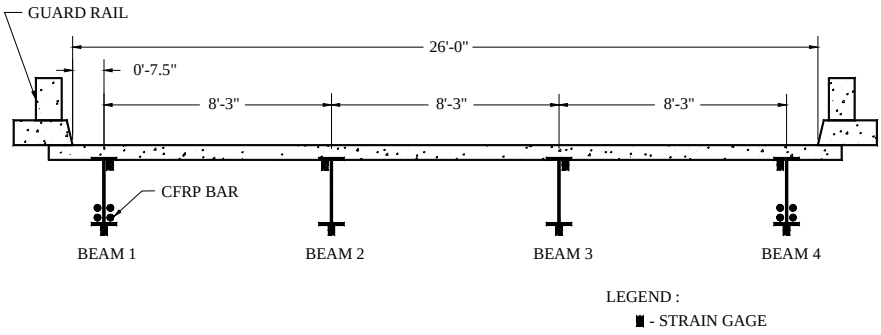

(b) Section A and C

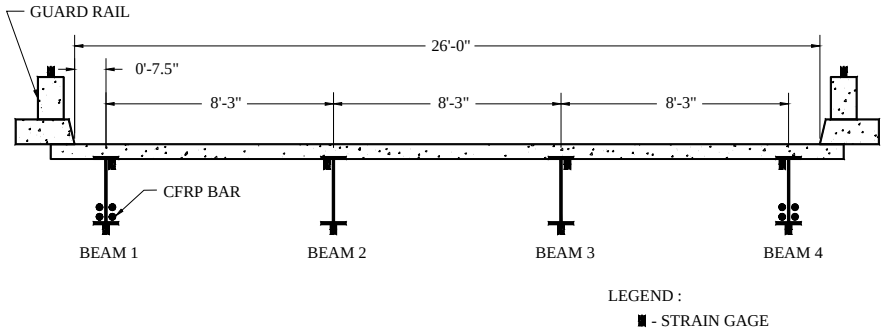

(c) Section B and D

Figure 16. Bridge strain gage locations and reference sections.

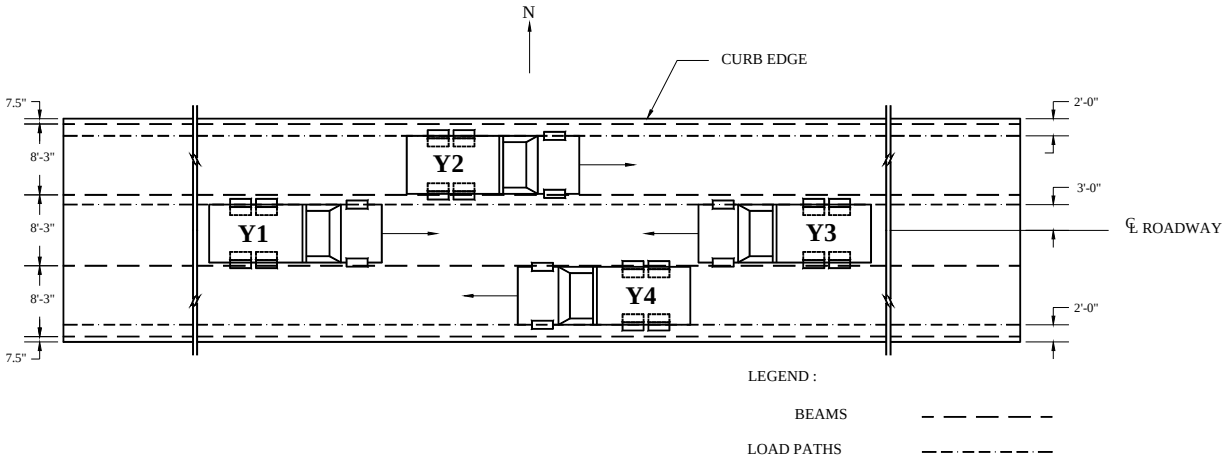

Figure 17. Truck paths used during load testing.

Figure 18. Photograph of typical load test truck.

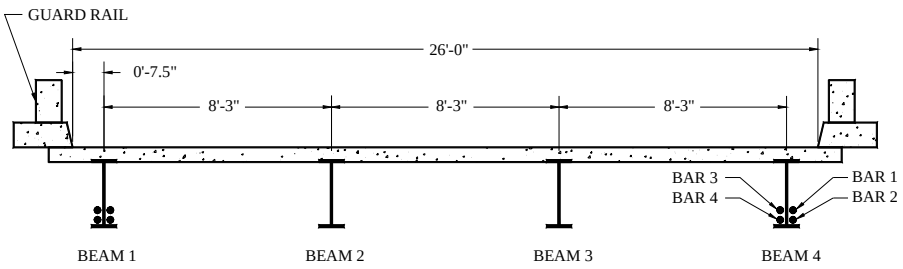

Figure 19. CFRP bars monitored during application of P-T force.

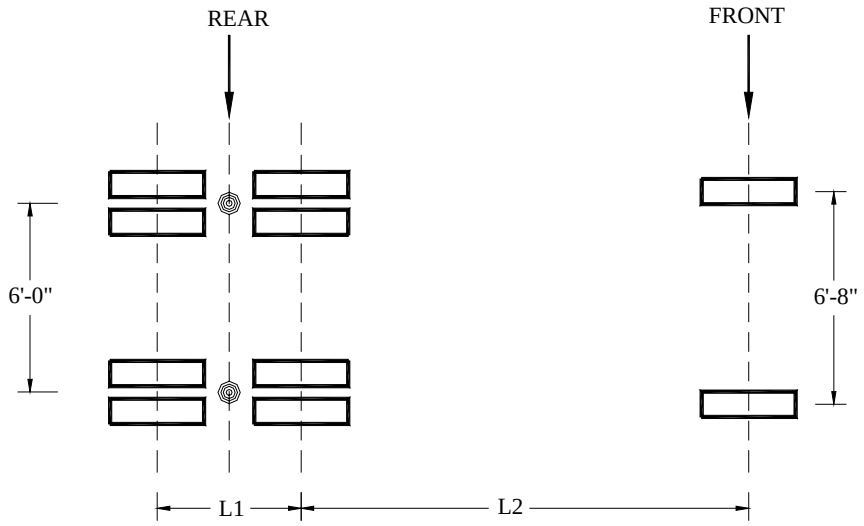

Figure 20. Dimension and weight of load truck.

Table 2. Summary of dimensions and weights of load truck.

Truck no.	L1	L2	Weight (lb)		
			Rear	Front	Total
1	4’-7”	14’-3”	39,520	16,400	55,920
2	4’-5”	14’-8”	37,420	14,740	52,160
3	4’-5”	14’-8”	36,680	12,520	49,200
4	4’-6”	15’-0”	32,280	13,200	45,600

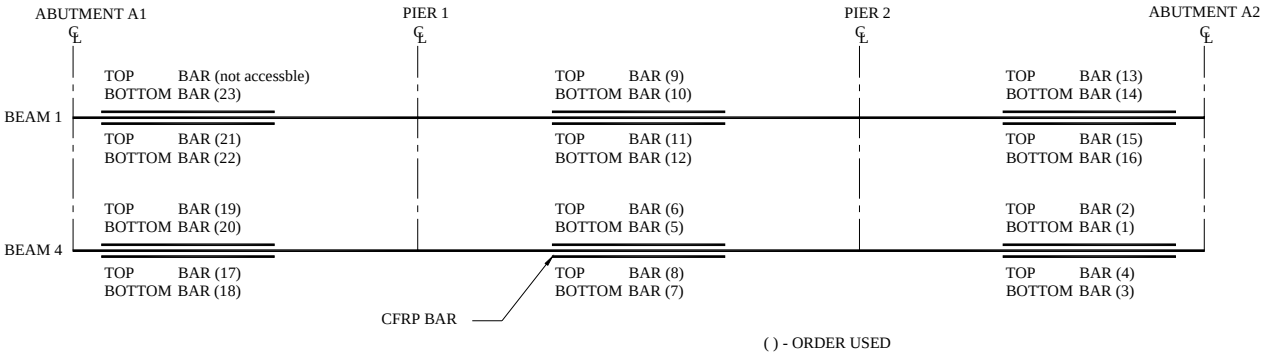

Figure 21. Order used in removing P-T force from each bar.

4. TEST RESULTS

Results from the various tests performed in the laboratory and in the field are presented in this chapter. Where applicable, the experimental results are compared with theoretical analysis results and mechanics based calculations.

4.1. Laboratory Test Results

As previously described, the 24-hour, constant load tests were conducted on three bars (S1, S2, and S3) and ultimate tensile strength tests on eight bars (S1 through S8) including the three bars tested under the 24-hour, constant load.

4.1.1. 24-Hour Constant Load Test Results

The constant load of 12 kips was applied to three of the specimens for 24 hours. After the 24 hours of loading, each specimen was removed from the test set up and thoroughly inspected. It was determined from visual inspection that no significant slip occurred during the period of this testing. As can be seen in Figure 22 and Table 3, which summarize the results of this testing, the maximum slip between the grip and the bar was less than 0.0011 in. in all cases. The fact that minimal slip was recorded, unfortunately, means that the source of slip observed in the field could not be determined.

Table 3. Summary of laboratory 24-hour constant load test results.

Specimen	Maximum slip (in.)	
	Top	Bottom
S1	0.0006	0.0007
S2	0.0005	0.0007
S3	0.0007	0.0011

4.1.2. Ultimate Strength Test Results

Ultimate tensile strength test was completed on all eight specimens (S1 through S8). As can be seen in Figure 23, it appears that all the CFRP bar specimens experienced several localized internal fiber failures (defined as peaks in Table 4) before the entire specimen failed. Each internal fiber failure can be identified as a significant stress decrease occurring at each peak in the plot. Based on “post-test” visual inspections of the failed specimens, it was found that failure of the specimens could be generally be grouped into three “modes.” Figure 24 shows typical examples of the three failure modes that were experienced in the ultimate strength test: tensile-rupture failure (Mode 1), grip-slip or pull-out failure (Mode 2), and combination failure (Mode 3). As can be seen in Table 5, five of eight specimens failed by pull-out (Mode 2).

In summary, the average stress and displacement of the specimen at the first peak were 241.9 ksi and 0.58 in., respectively, with the standard deviation of 68.0 ksi and 0.16 in.(see Table 4). Also, the maximum average stress and the maximum average displacement of the specimens at failure

were 344.5 ksi and 1.43 in., respectively, with the standard deviation of 14.9 ksi and 0.66 in. (see Table 5).

Although only a very small statistical sample was used in this test, the experimental data show minimal impact from the different loading rates used in the testing as described in section 3.1. The type of failure mode was also found to be unrelated to the ultimate strength of the CFRP bars. However, the specimens used in the 24-hour, constant load test seemed to exhibit higher stress levels at the first peak than the other specimens.

Although some of the specimens experienced internal breaks before they reached the specified ultimate strength (300 ksi) given by manufacturer, it appears from the test results that all specimens reached more than their full capacity.

4.2. Field Test Results

The bridge was tested for live load flexural response before and after the installation of the P-T strengthening system as previously described. Data were collected for the four different load paths shown previously in Figure 17. Recall also that the weights and dimension of the trucks used were given in Figure 20. For ease of interpretation, the data have been normalized based upon the total weight of the truck used in the initial test (i.e., subsequent test data were multiplied by the ratio of the initial test truck weight to the individual test truck weight) so that direct comparisons can be made.

In the following discussion, the longitudinal gage position will be referenced to Sections A through D that were shown in Figure 16. The following convention was adopted to describe the data in the subsequent figures. The notation starts with a letter "Y" followed by a number such as "Y1" to indicate the truck paths that were illustrated in Figure 17. This, in turn, is followed by another letter and a number such as "A1" to indicate a section location (i.e., "A") and a beam number (i.e., "1"). Finally, the notation is completed with a word such as "Top" or "Bottom" to indicate from where on the beam the data are recorded: top flange or bottom flange. For example, "Y2D3 Bottom" represents a data set collected from "Path Y2 - Section D - Beam 3 - Bottom flange." Some other notations used are described as follows:

- "Initial Test" : data set taken during "initial test" (Oct. 29, 2001).
- "t = 0 year" : data set taken during "immediately after installation test" (Nov. 9, 2001).
- "t = 1 year" : data set taken during "one year of service test" (Oct. 30, 2002).
- "t = 2 years" : data set taken during 'two years of service test" (June 11, 2003).

Note also that in figures showing "Truck Position," this is measured from the front wheel's location with respect to the bridge joints.

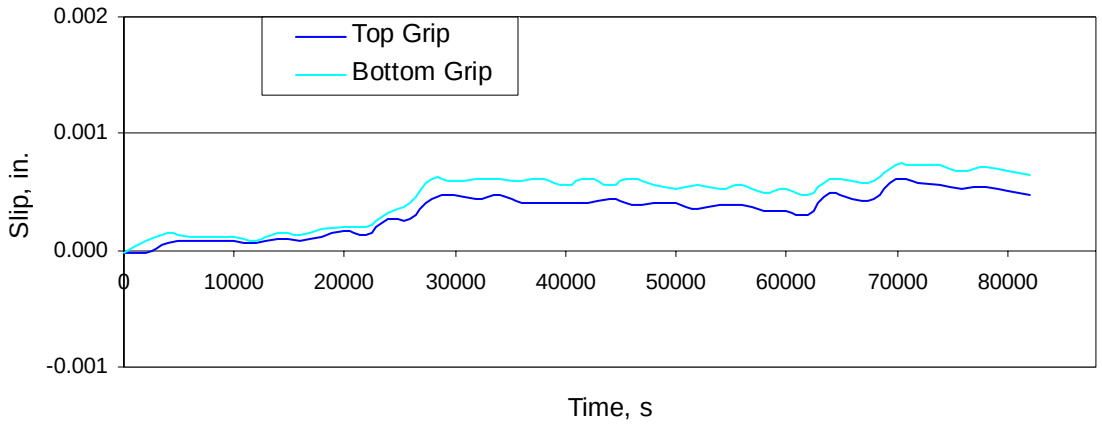

(a) Specimen 1 (S1)

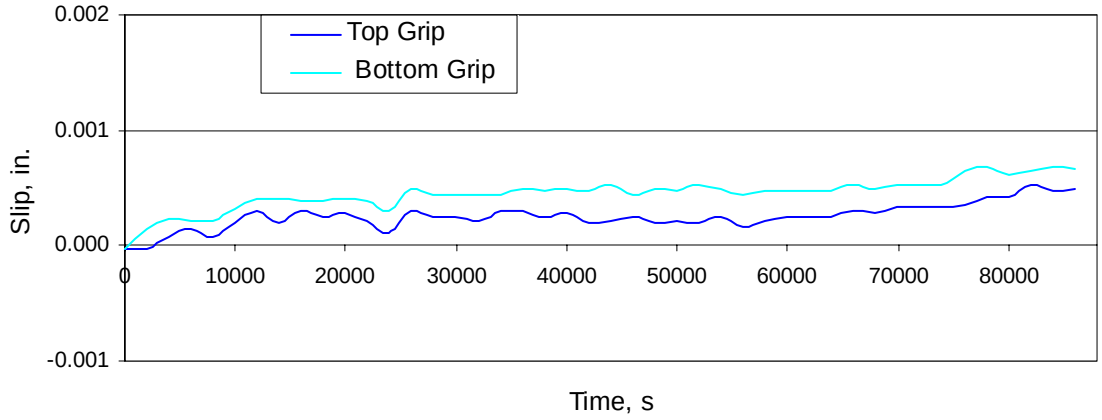

(b) Specimen 2 (S2)

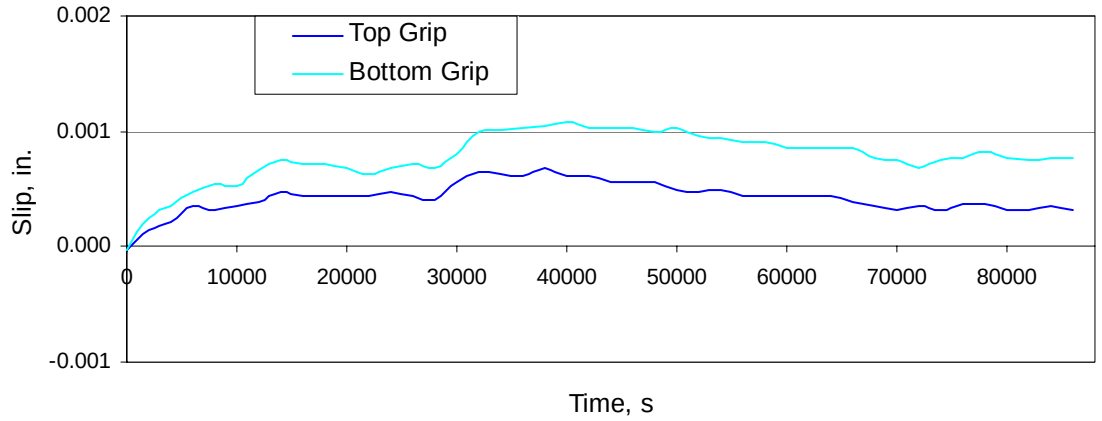

(c) Specimen 3 (S3)

Figure 22. Laboratory 24-hour constant load test results.

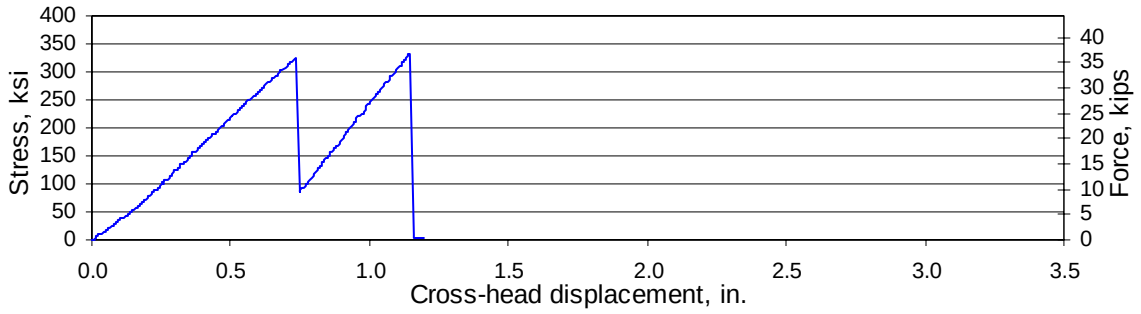

(a) Specimen 1 (S1)

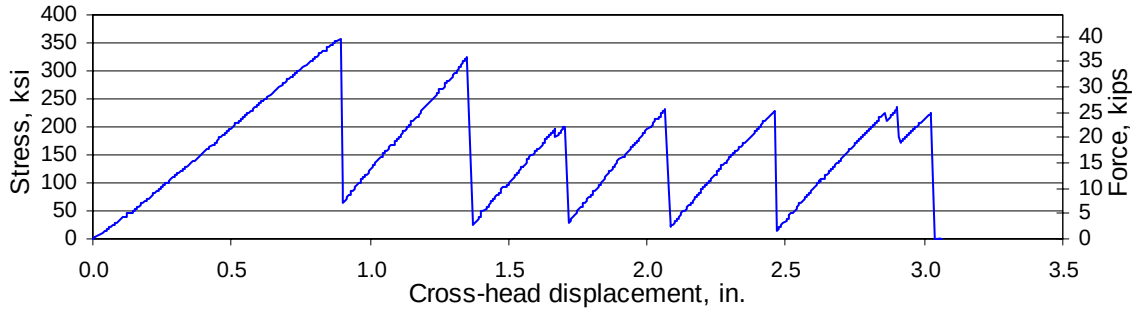

(b) Specimen 2 (S2)

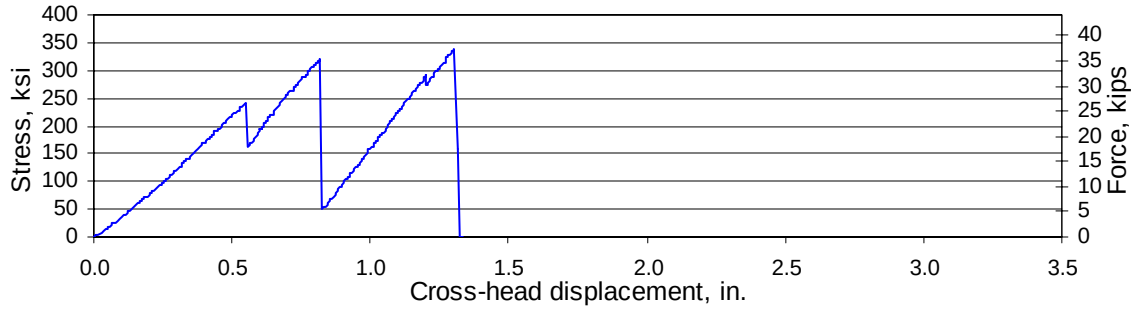

(c) Specimen 3 (S3)

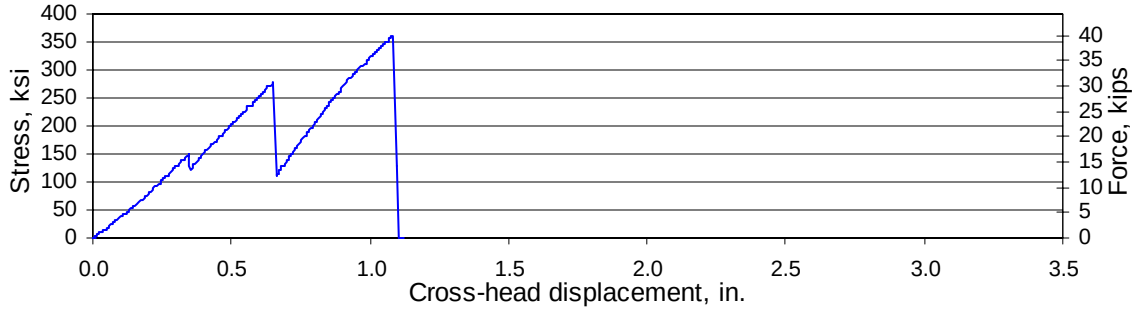

(d) Specimen 4 (S4)

Figure 23. Ultimate strength test results of laboratory specimen.

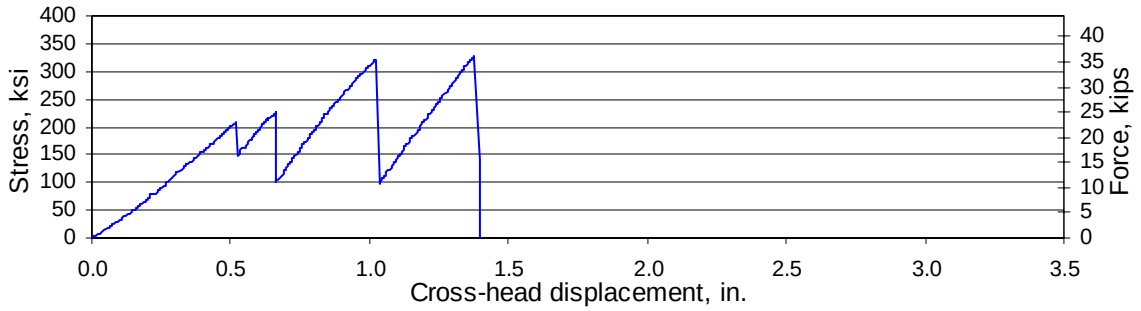

(e) Specimen 5 (S5)

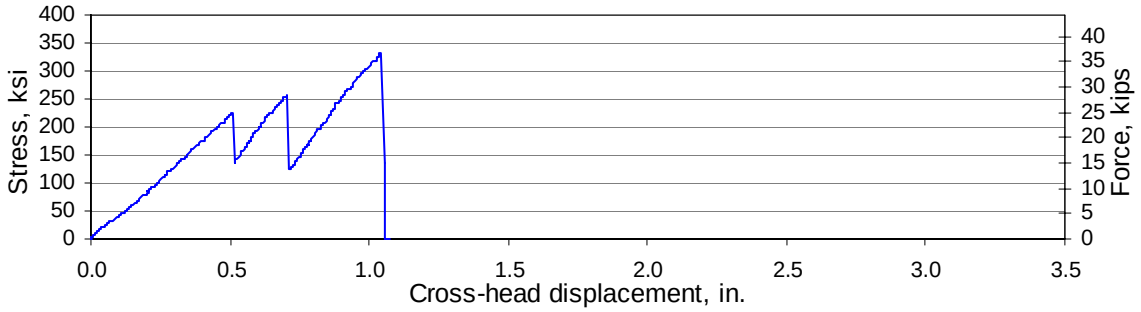

(f) Specimen 6 (S6)

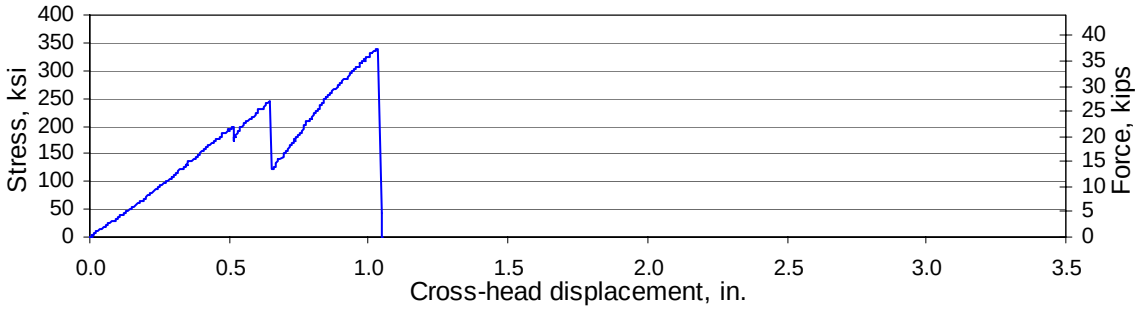

(g) Specimen 7 (S7)

(h) Specimen 8 (S8)

Figure 23. Ultimate strength test results of laboratory specimen (continued).

Table 4. Summary of laboratory specimen ultimate strength test result at first peak.

Specimen	Applied force at first peak (kips)	Stress at first peak (ksi)	Displacement at first peak (in.)
S1	36.0	326	0.734
S2	39.4	357	0.892
S3	26.6	241	0.549
S4	16.4	149	0.346
S5	22.9	208	0.519
S6	24.7	224	0.510
S7	21.9	199	0.514
S8	25.5	231	0.583

Table 5. Summary of laboratory specimen ultimate strength test result at failure.

Specimen	Total number of localized fiber failures before specimen failure	Stress at failure (ksi)	Displacement at failure (in.)	Failure mode
S1	2	332	1.143	1
S2	9	357	3.027	1
S3	4	339	1.303	3
S4	3	362	1.084	2
S5	4	328	1.377	2
S6	3	332	1.042	2
S7	3	340	1.033	2
S8	4	366	1.396	2

(a) Failure mode 1 (tensile-rupture)

(b) Failure mode 2 (pull-out)

(c) Failure mode 3 (combination)

Figure 24. Laboratory specimen failure modes.

4.2.1. Initial Test

As previously mentioned, an initial diagnostic load test was conducted prior to the installation of the P-T strengthening system to establish a baseline static behavior of the unstrengthened bridge. The goal of this testing was to understand the general, global behavior of the bridge and to ensure that any future changes in behavior could be identified.

In general, all collected strains showed an elastic response (i.e., strains from all gages returned to zero after each truck crossed the bridge). The neutral axis location was found to generally be close to the top flange in the positive moment region, thereby verifying the composite behavior of the beam. By observing flexural tensile and compressive strains measured at Section A (near Abutment A1) and their relative magnitudes with respect to midspan strains, as shown in Figures 25 and 26, it was observed that some rotational end restraint is present at the abutment. This unintended rotational restraint could be attributed to corrosion of the abutment bearings (see Figure 1), accumulation of debris, and the presence of a heavy diaphragm over the abutment bearings. In addition, the strain patterns show a symmetric response that corresponds to the symmetrical nature of the bridge and the truck paths utilized. For example, strains due to truck paths Y1 and Y3 on Beam 2 and Beam 3 (or Beam 1 and Beam 4), respectively, exhibited a similar, symmetrical behavior as is shown in Figure 26b. In general, strains in the positive moment regions exhibited a higher degree of symmetry than in the negative moment region. Some of the slight differences in transverse behavior may be attributed to differences in local stiffness and/or possible experimental error (e.g., differences in truck wheel line distribution, lateral truck positioning, etc.).

4.2.2. Influence of Post-tensioning Strengthening System on Live-load Response

This section describes the response and behavior of the bridge tested after the installation of the P-T strengthening by comparing strain measurements from each test. Recall that the gage locations and truck paths used were shown in Figure 16 and 17. In the interest of brevity, only bottom flange strains will be presented in this section. However, it should be pointed out that the top flange generally exhibited the same behavior.

Follow-up load tests (immediately after installation, one year of service, and two years of service) were carried out on the post-tensioned bridge to investigate the bridge's behavior before and after the P-T strengthening system installation. Typical strain data from these tests are illustrated in Figures 27 through 30. From the follow-up test results, several important observations were made. Each load test produced fairly consistent strain readings with those established during the initial test. This consistency in strain is informative in that it indicates that the P-T system did not significantly alter the behavior of the bridge over the two years of service, as would be expected. Although it is not possible to precisely account for all the sources of strain, it is evident from the consistency of the strain data that the installation of the P-T system had negligible impact on changing the stiffness of the bridge. The data also indicate that the live load distribution characteristics are virtually the same before and after the installation of the P-T system. In general, good agreements in strain data were observed; however, there were some relatively small discrepancies observed at several locations. These discrepancies may be the result of

- Changes in end restraint due to application of the P-T force;
- Inadvertent variations in truck positions and geometry.

4.2.3. During Post-tensioning

As mentioned in Chapter 3, during the application of the P-T force, the bridge and the P-T strengthening system were monitored. The behavior of the bridge during the application of the P-T force will be presented in the following sections.

4.2.3.1. STRAIN INCRESE DURING POST-TENSIONING

Proper P-T in the positive moment region generates strain opposite in sign to those produced by dead and live loads. During the application of the P-T strengthening system, strain was measured to investigate the response of the bridge due to the applied P-T force. As expected, when the force was applied to a specific location, that specific beam would experience the greatest change in strain. For example, when the north exterior beam (Beam 1) in the west end span was post-tensioned (events 17 through 32 in Figure 31), the strain due to the P-T force increased significantly compared to other locations where increases in strain were minimal. Likewise, significant increase in strain can be observed during P-T on Beam 1 in the center span (Events 49 through 64 in Figure 32). However, it should be noted that a non-trivial level of strain was measured at other locations as well.

4.2.3.2. LATERAL DISTRIBUTION

As was mentioned in the previous section, notable amounts of P-T induced strain were recorded at locations away from the applied P-T force. This section investigates the lateral distribution of the P-T force on the bridge. Shown in Figure 33 is an overall distribution pattern of the bridge at each section with Beam 1 in each span being post-tensioned. From these figures, it is clear that the effects of the P-T system are distributed throughout the bridge. It is likely that the amount of P-T force distributed is highly dependent upon the deck and diaphragm stiffnesses.

The lateral load distribution can be expressed as a percentage of the P-T force remaining on each beam. Since the exterior beams and the interior beams have different material and section properties, the distribution factor of the individual beams during P-T Beam 1 in the west end span and the center span (referred to as “WSB1” and “CSB1,” respectively, in Table 6) were determined based on the expression presented below. Note that the modulus of elasticity (E) on the exterior and interior beam was assumed to be constant.

$$\%\ DF_i = \frac{\varepsilon_i S_i E_i}{\sum\left(E_i \varepsilon_i S_i\right)} * 100 = \frac{\varepsilon_i S_i}{\sum\left(\varepsilon_i S_i\right)} * 100\ , \qquad (4.1)$$

where

ε_i = bottom flange strain due to P-T in i^{th} beam.
S_i = section modulus of i^{th} beam.
E_i = modulus of elasticity.

With the above equation, the lateral distribution was determined to be, on average, 58% on Beam 1, 27% on Beam 2, and 15% on Beam 3. It was also found that the application of P-T force on one exterior beam (e.g., Beam 1) has a negligible impact (nearly 0%) on the other exterior beam (e.g., Beam 4). These lateral distributions characteristics are summarized in Table 6.

From the data presented in Table 6 and assuming a fairly symmetric response, it was determined that 58% of the P-T force would act on each exterior girder and that 42% would act on each interior girder.

4.2.3.3. VERIFICATION OF POST-TENSIONING FORCE

In order to verify the level of force applied by the P-T strengthening system in the field, a calibration was performed, in the laboratory, on four of the CFRP bars that were to be installed on Beam 4 in the west end span. The strain data measured during the application of P-T force to each of these bars (Events 1 through 16) are shown in Figure 34 where each event defines a specific step of the P-T process, as previously described.

From these data and the laboratory calibration, the actual forces in each bar during P-T application could be determined. As summarized in Table 7, all bars are slightly under-tensioned. Bars 1 and 2 were under-tensioned by 10.8%, and Bars 3 and 4 were under-tensioned by 15.8% and 11.6%, respectively. Also, note that the force in each bar changed as force was applied to other bars. The final force in each bar after all four bars at this location had been tensioned was 10.7 kips (Bars 1 and 2), 10.1 kips (Bar 3), and 10.6 kips (Bar 4). By adding the force applied to each bar, it was determined that the total of 42.2 kips were actually applied on Beam 4 in the west end span.

In the previous section, a general study of how P-T forces are laterally distributed was discussed. In an effort to account for longitudinal distribution, an analysis utilizing STAAD Pro. was conducted. Based on this analysis, it was found that approximately 10% of the P-T force applied on the exterior girder in the end span (P-T force being applied only to one location) is longitudinally distributed.

Likewise, 27.5% of the P-T force on the exterior beam in the center span is longitudinally distributed to other spans (13.8% to each adjacent span). Having accounted for these longitudinal distributions, the “remaining P-T force” at each section could be determined; a product of 42.2 kips and percentage of the longitudinal distribution of the P-T force (38.0 kips at Section B and 30.6 kips at Section D). Following this, an attempt was made through mechanics principles to account for all of the P-T force. To accomplish this, a relatively simple mathematical model (see Figure 35) was developed to represent the beams during P-T application. From this model and the measured strain, discrete forces acting at each location were estimated. The sum of these discrete forces was then compared to the computed “remaining P-T force.”

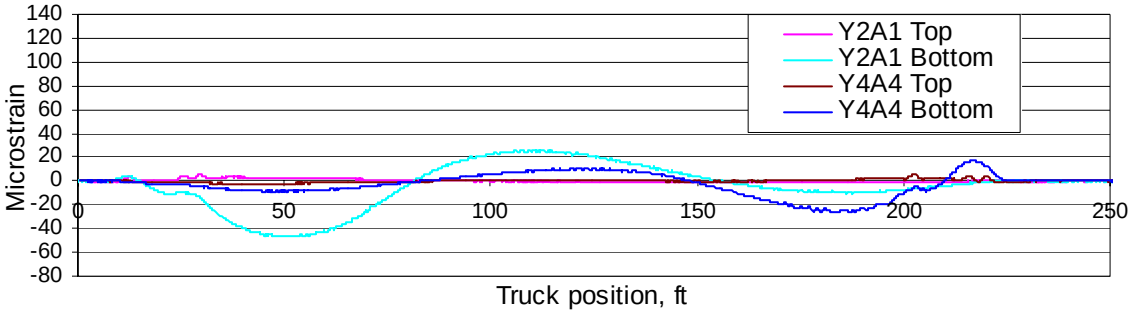

(a) Section A

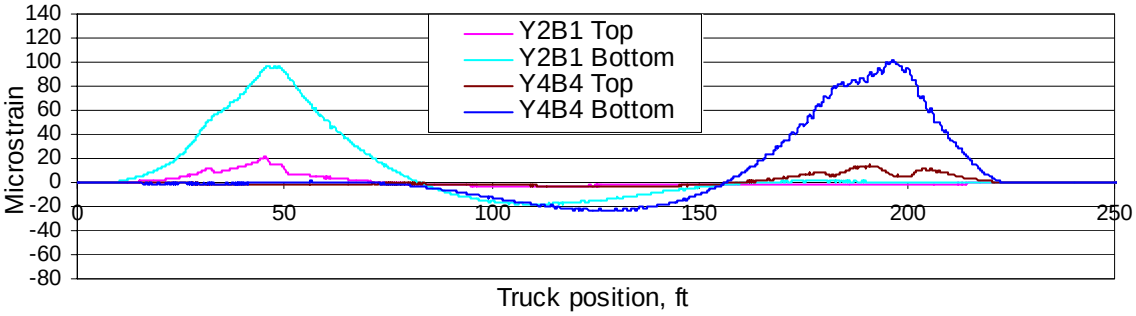

(b) Section B

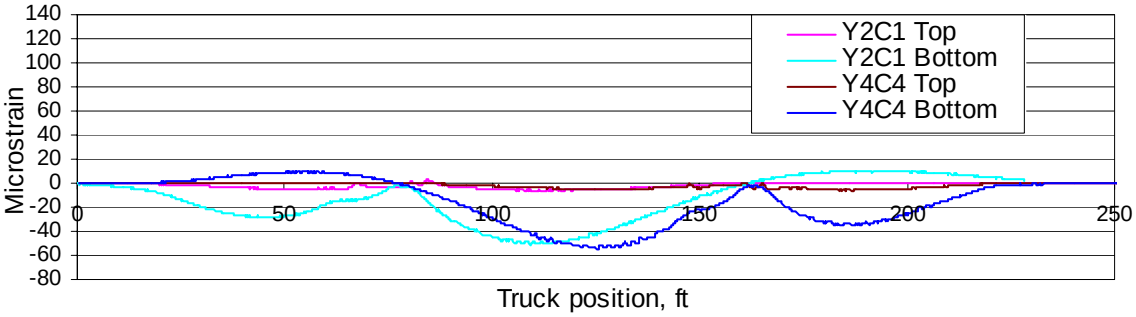

(c) Section C

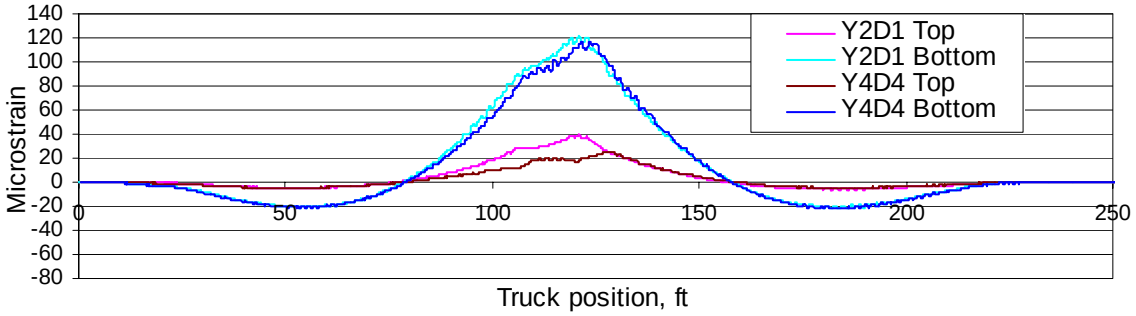

(d) Section D

Figure 25. Before strengthening: Strains in Beam 1 (path Y2) and Beam 4 (path Y4).

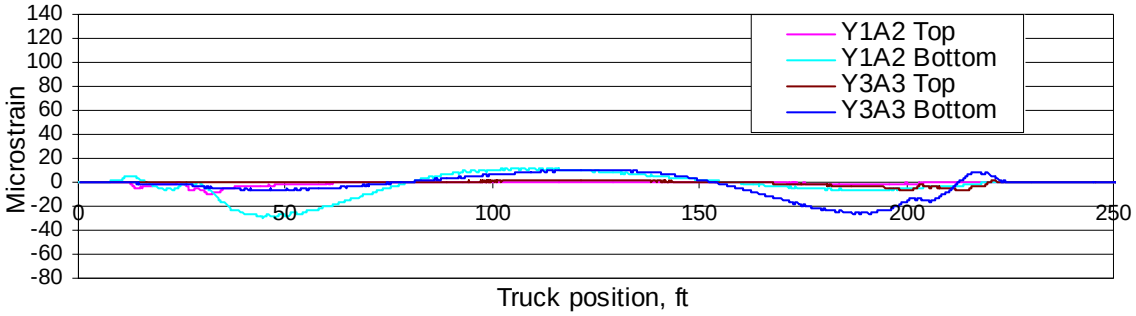

(a) Section A

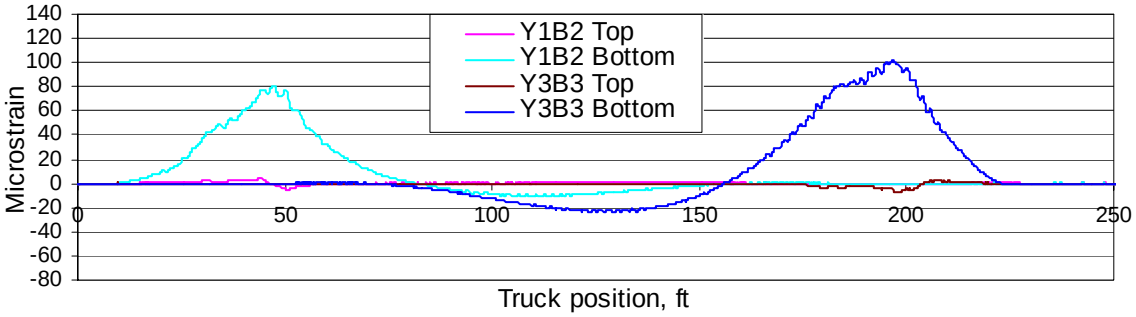

(b) Section B

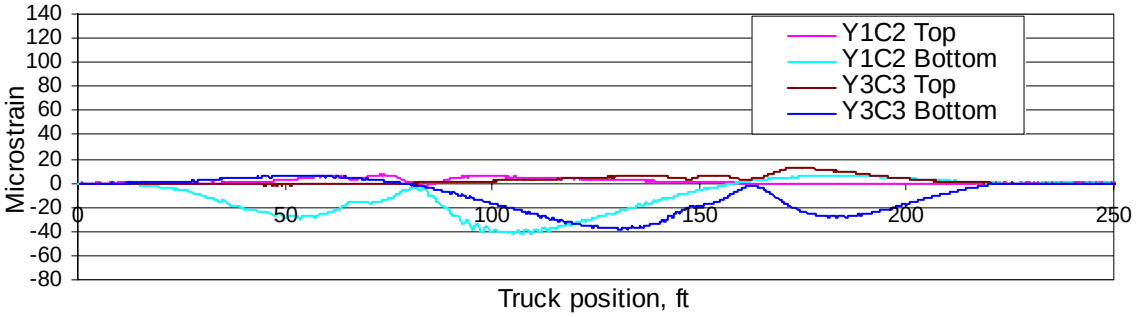

(c) Section C

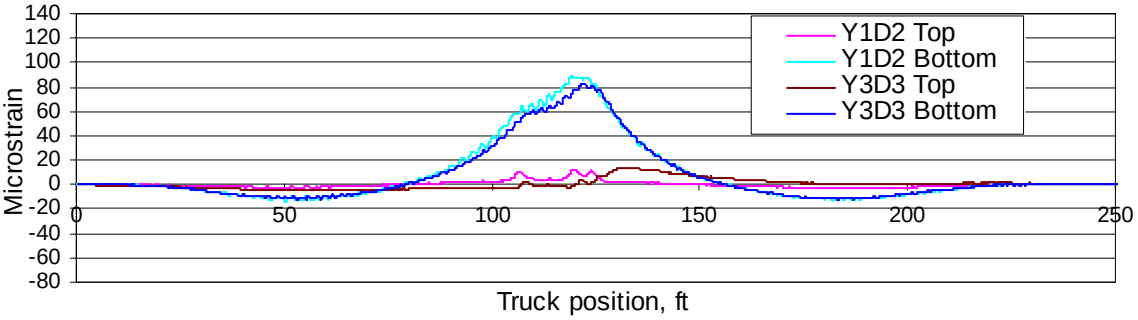

(d) Section D

Figure 26. Before strengthening: Strains in Beam 2 (path Y1) and Beam 3 (path Y3).

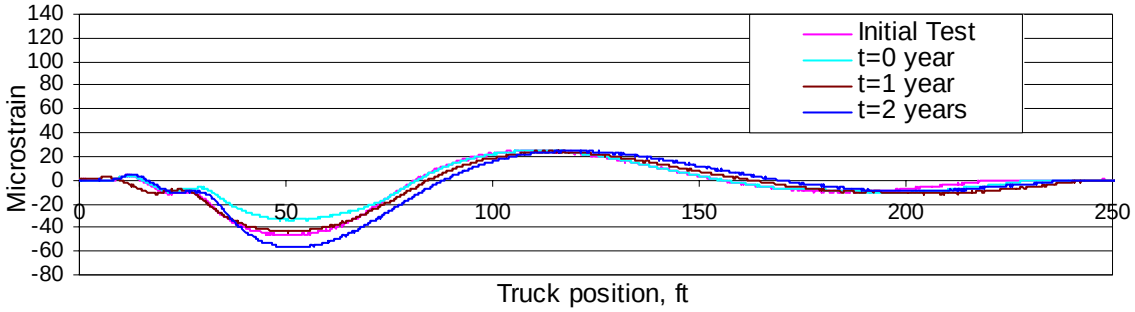

(a) Section A

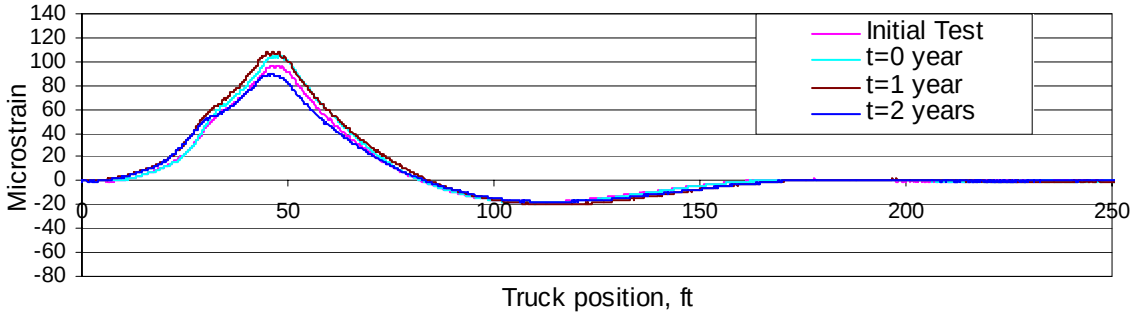

(b) Section B

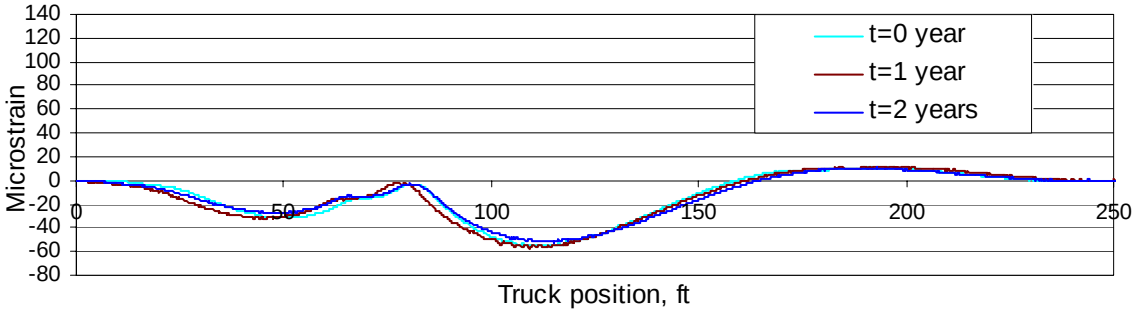

(c) Section C

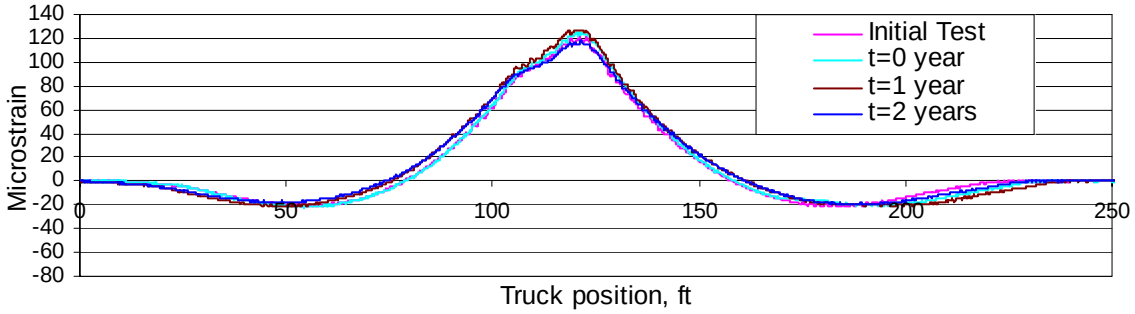

(d) Section D

Figure 27. Before and after strengthening: Strains in Beam 1 (path Y2).

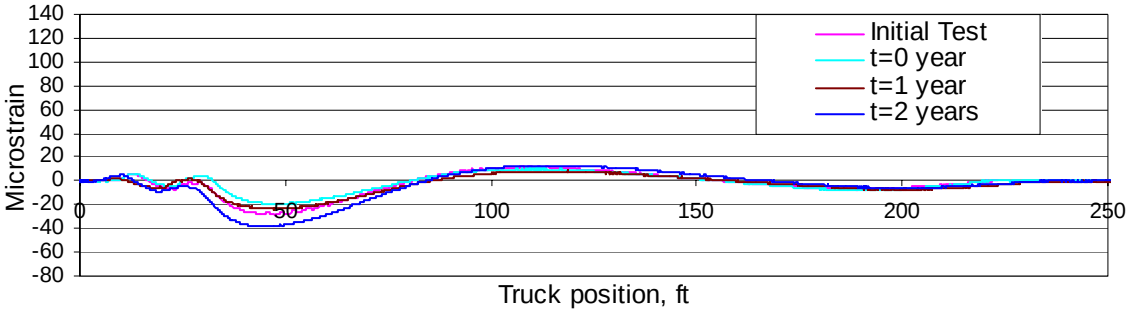

(a) Section A

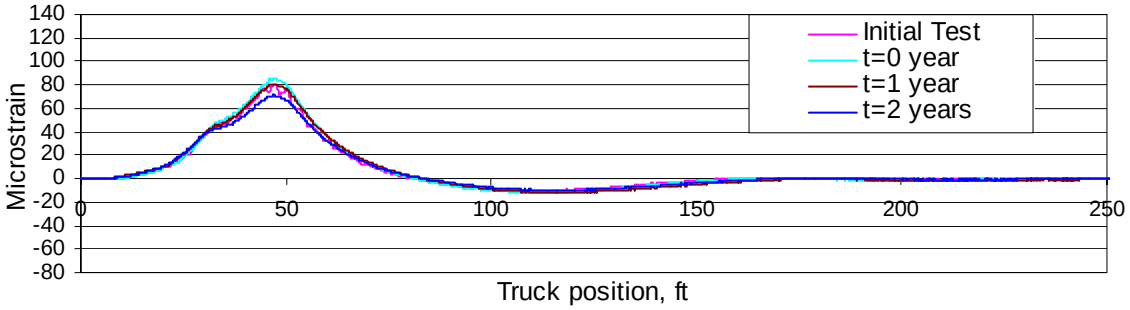

(b) Section B

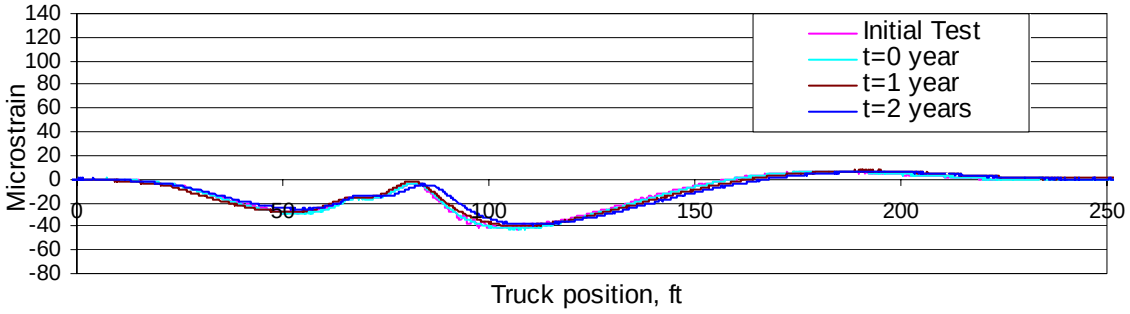

(c) Section C

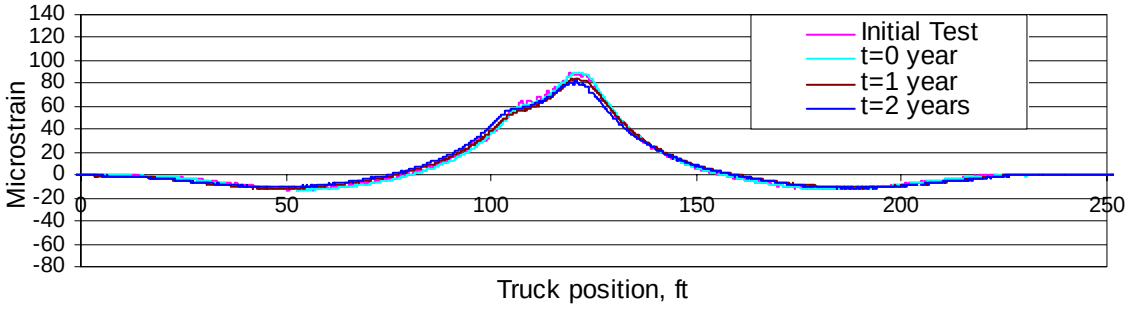

(d) Section D

Figure 28. Before and after strengthening: Strains in Beam 2 (path Y1).

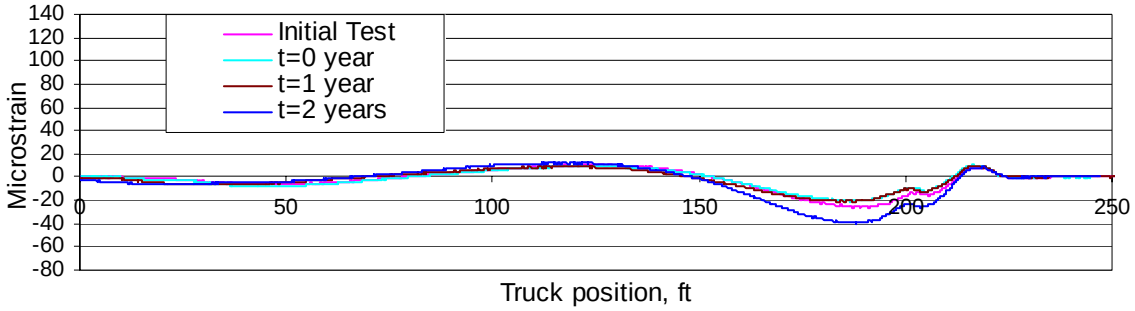

(a) Section A

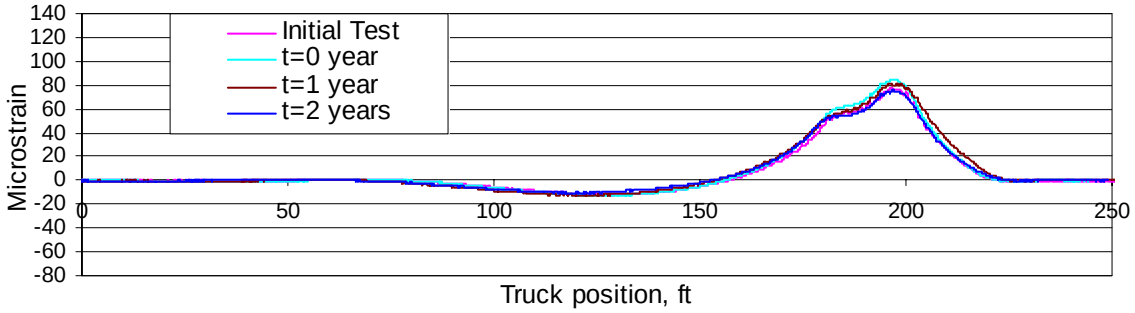

(b) Section B

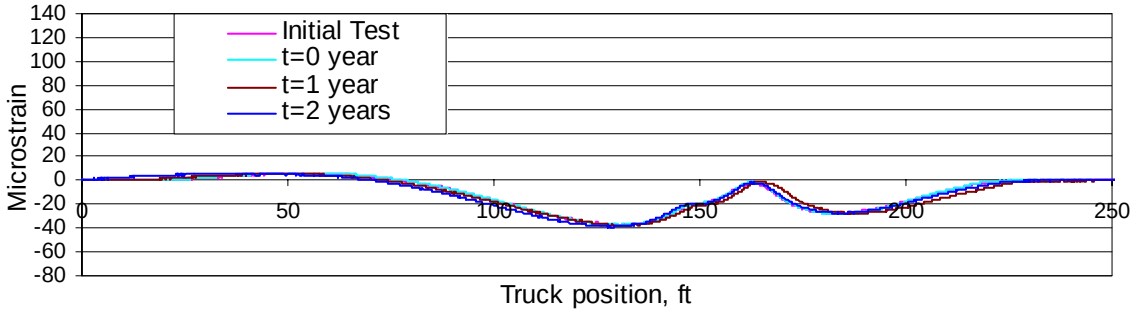

(c) Section C

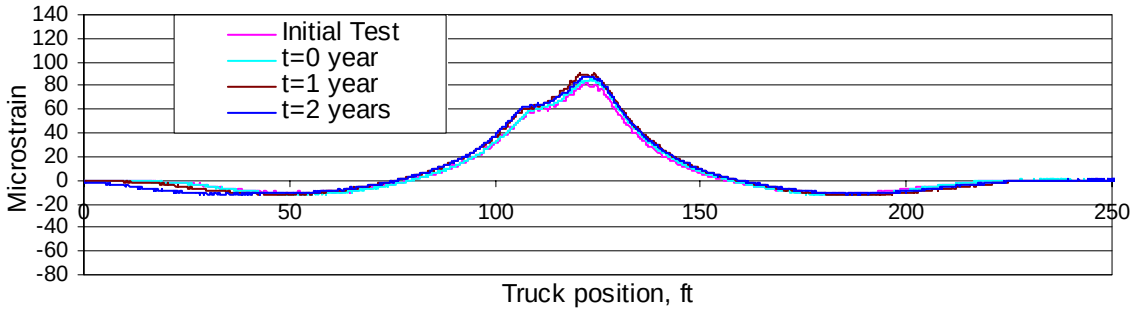

(d) Section D

Figure 29. Before and after strengthening: Strains in Beam 3 (path Y3).

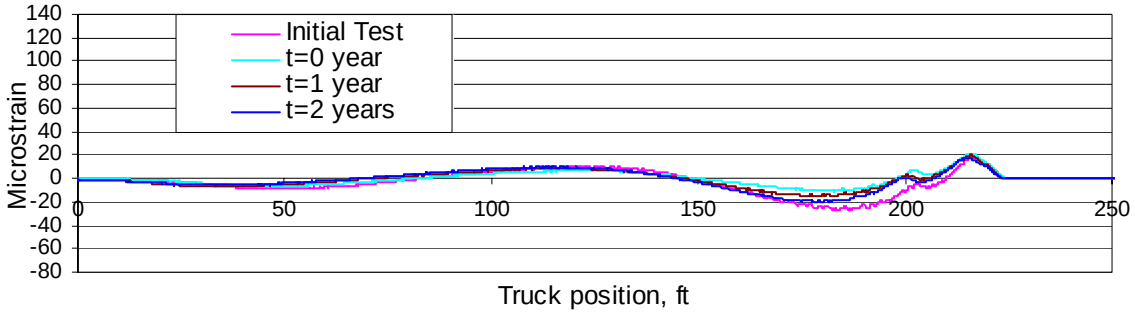

(a) Section A

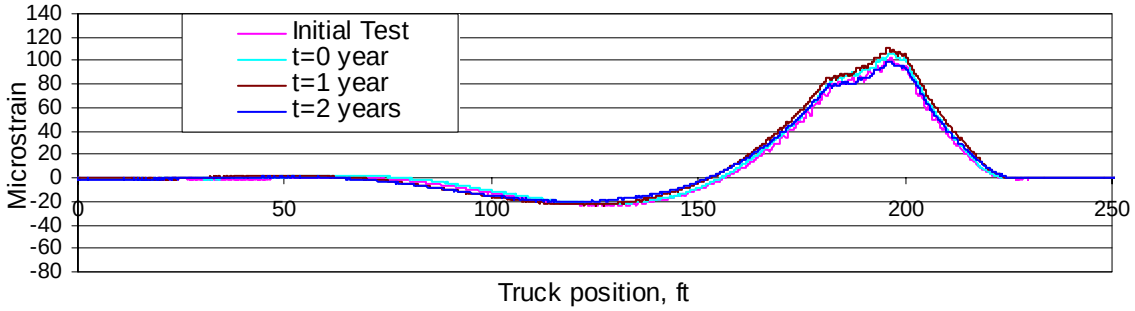

(b) Section B

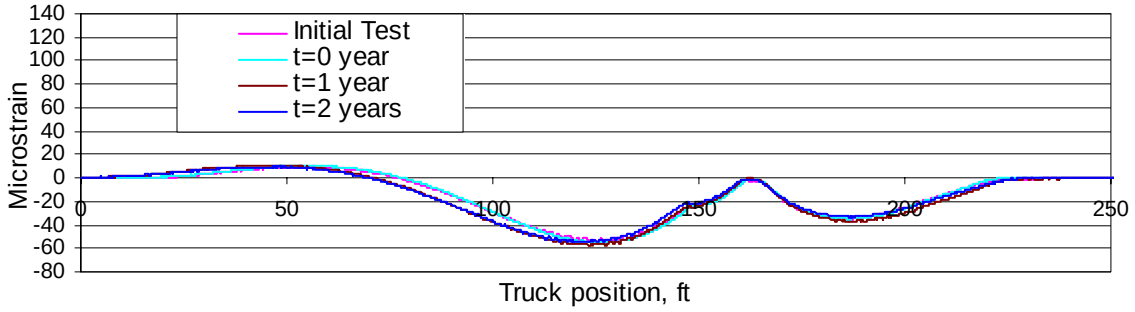

(c) Section C

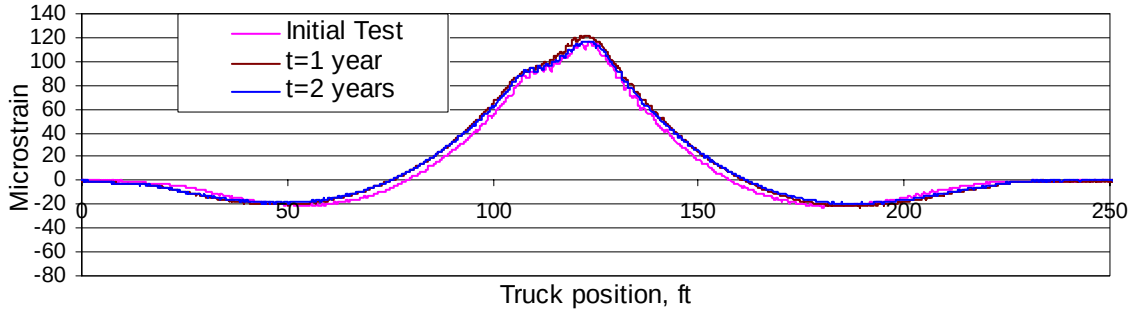

(d) Section D

Figure 30. Before and after strengthening: strains in Beam 4 (path Y4).

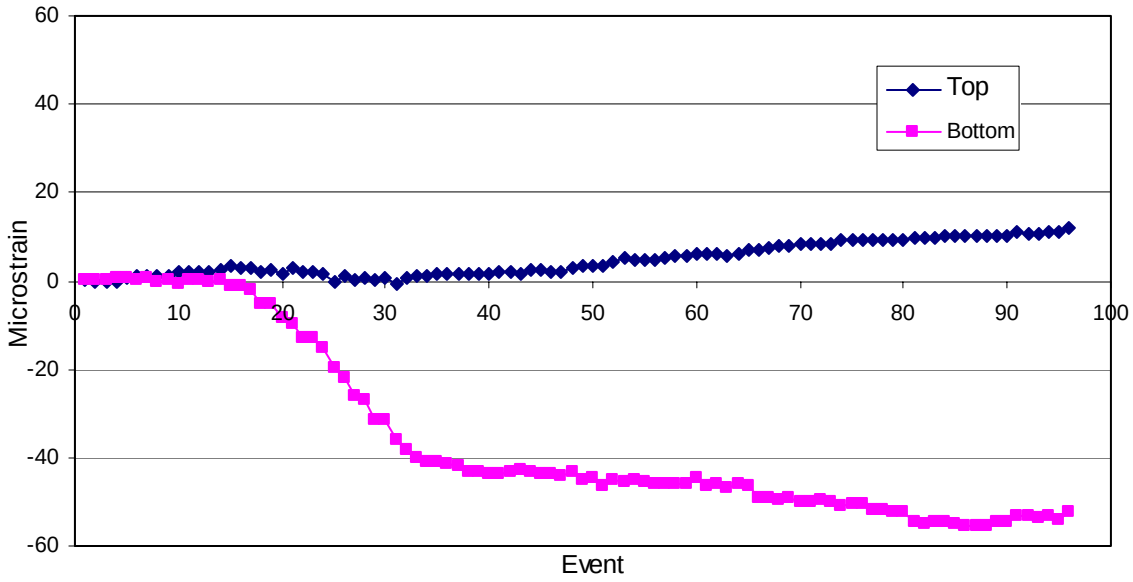

Figure 31. Strains measured in west end span, Beam 1 during P-T.

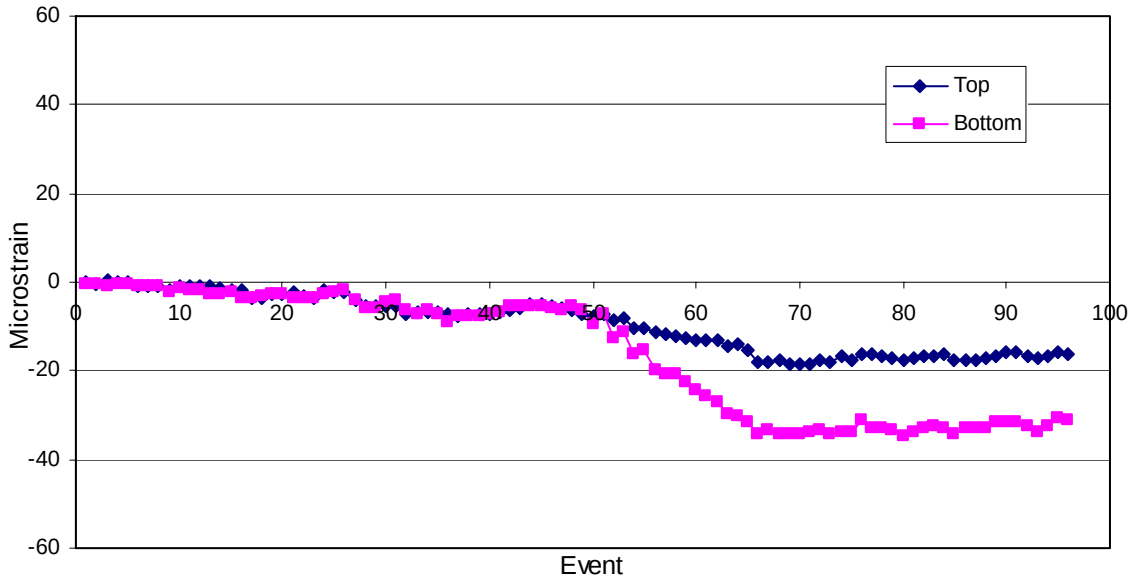

Figure 32. Strains measured in center span, Beam 1 during P-T.

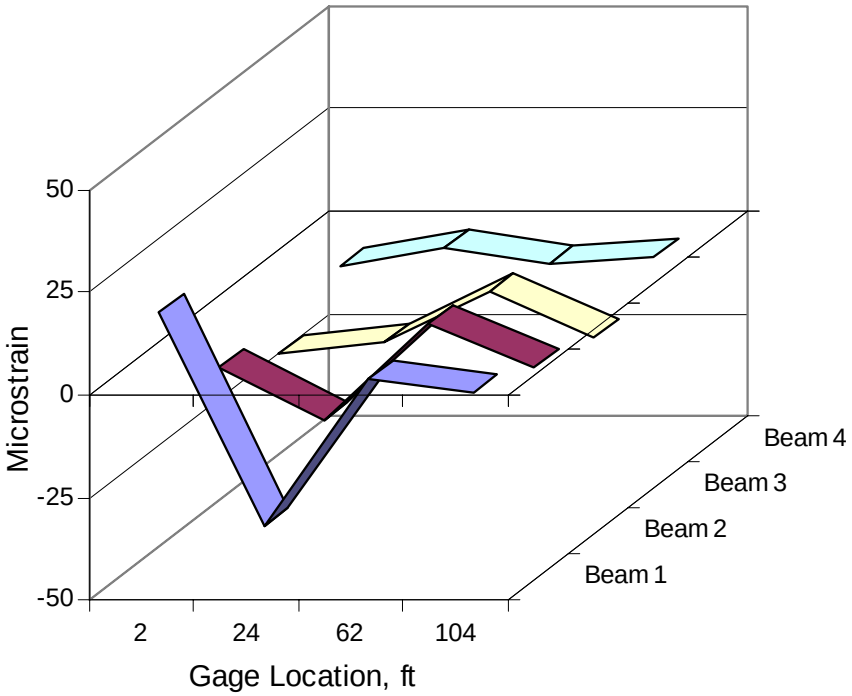

(a) P-T force applied to west end span Beam 1 (Events 17-32)

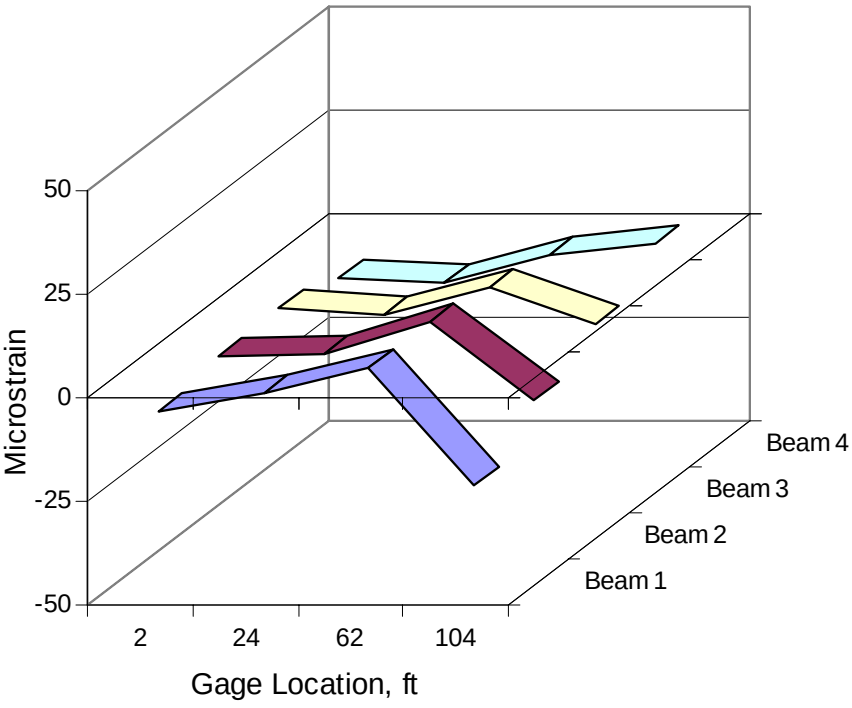

(b) P-T force applied to center span Beam 1 (Events 49-64)

Figure 33. Distribution of P-T strains.

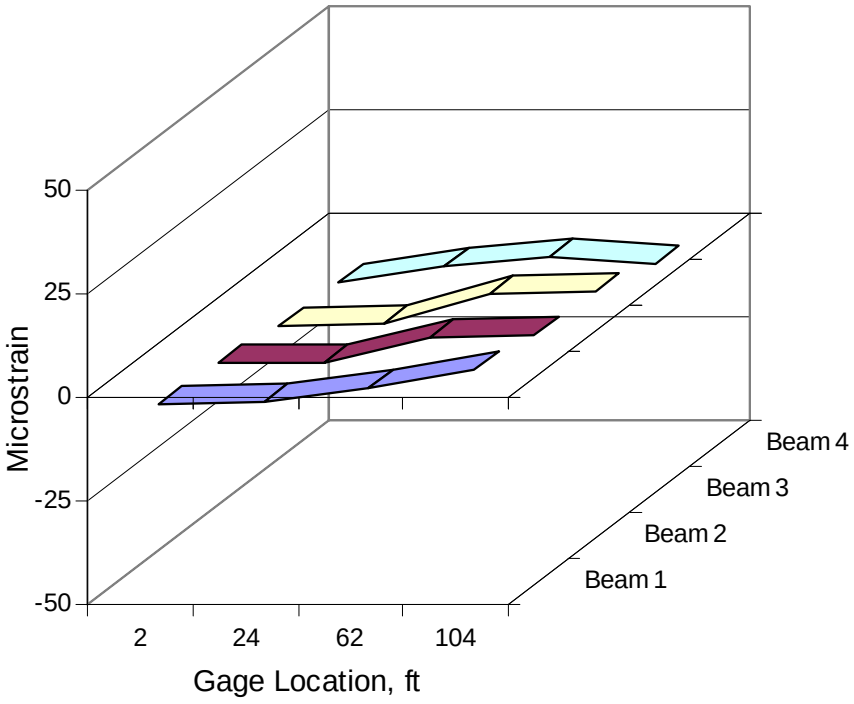

(c) P-T force applied to east end span Beam 1 (Events 81-96)

Figure 33. Distribution of P-T strains (continued).

Table 6. Lateral distribution of bottom flange strain during P-T on Beam 1.

	% of bottom strains			
	Beam 1	**Beam 2**	**Beam 3**	**Beam 4**
During P-T of WSB1	57	26	16	1
During P-T of CSB1	59	28	14	-1
Average	58	27	15	0

Table 7. Summary of P-T forces in bars on west end span, Beam 4.

	Bar 1		**Bar 2**		**Bar 3**		**Bar 4**	
Event	**(4)**	**(14)**	**(2)**	**(12)**	**(7)**	**(9)**	**(6)**	**(10)**
Strain, με	2,445	4,855	2,460	4,850	0	4,590	2,510	4,815
Intended force, kips	6	12	6	12	6	12	6	12
Applied force, kips	5.4	10.7	5.4	10.7	0	10.1	5.5	10.6
% of under-tensioned		10.8		10.8		15.8		11.6

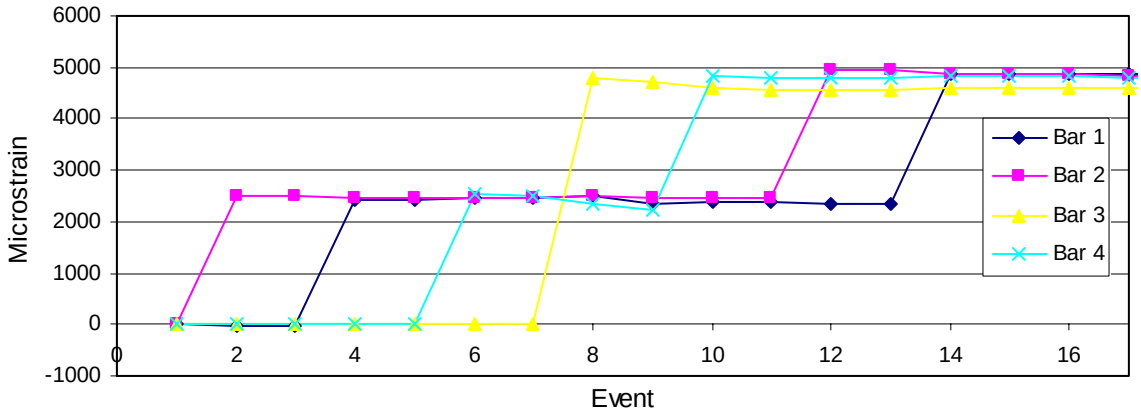

Figure 34. Bar strains resulting from P-T west end span, Beam 4.

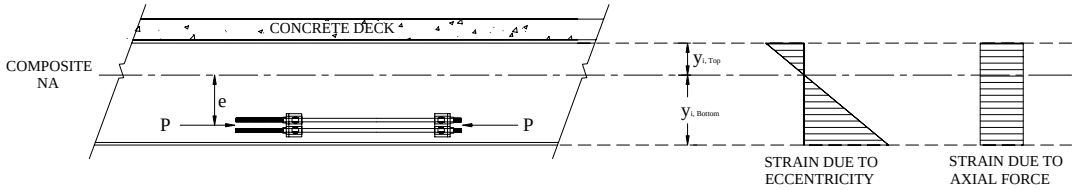

(a) Applied P-T force and corresponding strain diagrams

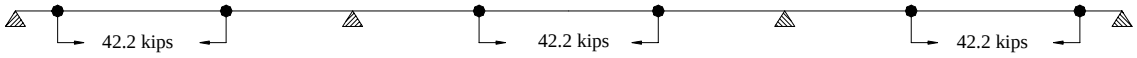

(b) Idealized beam with eccentric forces

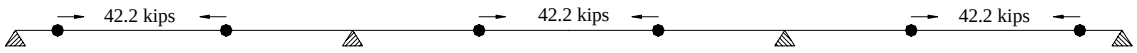

(c) Idealized beam with axial forces

(d) Idealized beam with moment forces

Figure 35. Idealized beams with applied forces.

The mathematical model used is illustrated in Figure 35 where the application of an eccentric P-T force can be resolved into 42.2 kips of a concentric axial force and 100 ft-kips of applied moment (42.2 kips at an eccentricity, e, of 28.4 in.).

A total strain can be expressed as a sum of strains due to an axial force and moment that is a product of the axial force and the eccentricity.

$$\varepsilon_{Total} = \pm \frac{Pey}{EI} \pm \frac{P}{AE}, \tag{4.2}$$

where

P = applied P-T force.
e = eccentricity (distance between axial force and composite NA).
y = distance from composite NA to bottom flange gage.
E = modulus of elasticity of beam.
I = moment of inertia.
A = cross sectional area of composite beam.

This equation can be re-written and solved for the discrete force acting on each individual beam.

$$P_i = \frac{\varepsilon_i}{\frac{ey_i}{EI_i} - \frac{1}{EA_i}}, \tag{4.3}$$

where

P_i = P-T force acting on i^{th} beam.
ε_i = strain obtained from i^{th} beam.
y_i = distance from composite NA to bottom flange on i^{th} beam.
I_i = moment of inertia of i^{th} beam.
A_i = cross sectional area of i^{th} beam.

Now, the sum of the discrete force on each beam can be determined.

$$P_{Total} = \sum P_i \tag{4.4}$$

Using the relationships presented above and the measured strain data, the discrete force acting on each beam was determined. Results at Section B and Section D are shown in Figure 36 and summarized in Table 8.

With higher percentage difference in the west end span, it was generally found that the sum of the discrete forces computed based on the experimental strains were higher in the west end span and lower in the center span than the “remaining P-T force.”

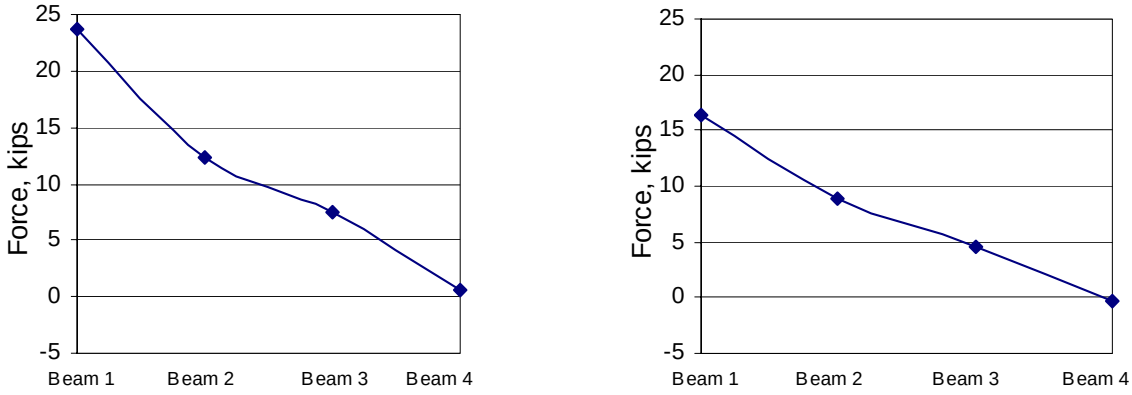

(a) P-T in west end span Beam 1 (b) P-T in center span Beam 1

Figure 36. Discrete forces acting on each beam.

Table 8. Summary of discrete force acting on each beam.

	Discrete force acting on each beam (kips) Beam 1 + Beam 2 + Beam 3 + Beam 4				=	Sum of discrete force (kips)	Remaining P-T force (kips)	% Difference
Section B during P-T WSB1	23.6	12.4	7.5	0.6	=	42.8	38	11.2
Section D during P-T CSB1	16.5	8.9	4.6	-0.3	=	28.7	30.6	-6.6

4.2.4. Effect of Post-tensioning

As stated previously, the goal of the P-T strengthening system is to create an effective way of introducing stresses in the bridge that counteract the stresses produced by dead and live loads. The impact of the P-T strengthening system on individual beams as well as the entire bridge will be discussed in following sections.

4.2.4.1. ANALYTICAL MODELING

A mathematical model was developed to better understand the impact of the P-T strengthening system by investigating the overall behavior of the bridge due to P-T force application. To accomplish this, a grillage model was developed to study the global behavior. Where possible, results from this model are compared with the field test results.

4.2.4.1.1. Grillage Modeling

A model was developed using a commercially available structural analysis package. Due to the difficulty in quantifying end restraint, all supports were modeled as rotationally free. As was used in the model shown in Figure 35, a concentric axial force and an applied couple were used in this analysis to simulate the eccentric P-T force acting on the bridge.

To facilitate the analysis, several assumptions were made:

- The steel and concrete deck are perfectly connected by means of shear connector; thus, the beams behave compositely, acting as a homogeneous section. Computations are based on full interaction without slip between concrete deck and steel beam.
- Section properties of the analytical model are constant along the beam.
- Difference in elastic properties between the concrete deck and steel beam can be properly adjusted through the use of an elastic modular ratio based on AASHTO Standard Specification [10].
- Stiffness contribution of CFRP bars to composite beam is negligible and thus not included.
- Partial end restraints at the abutment were neglected.

4.2.4.1.2. Illustration of Post-tensioning Effect

The construction sequence for the application of P-T forces was documented in section 2.2.2. In order to better understand how the bridge behaves during the application of the P-T strengthening system, the same application sequence was applied in the grillage model. The resulting internal moment diagrams are shown in Figure 37.

From this analysis, it appears that the P-T strengthening system impacts both the positive and negative moment regions by producing moments opposite in sign to those induced by dead and live loads. Note that for the exterior beams, the larger moment was generated at the anchorage locations rather than at midspan region (i.e., maximum positive moment region). A different pattern, however, was observed on the interior beams; the effect of the P-T strengthening system is the highest near the maximum positive moment location. The grillage analysis also verified that significant P-T forces could be distributed to adjacent beam. It was also observed that larger moments were generated in the end spans than in the center span.

4.2.4.1.3. Comparison of Lateral Distribution During P-T

The theoretical bottom flange strain distribution at Sections B and D during the P-T process was determined from the grillage analysis. These analytical results were then compared with the experimentally determined lateral load distribution characteristics previously presented.

From the grillage analysis, it was found that, on average, when Beam 1 was post-tensioned, 52% of the total strain occurred in Beam 1 while 31%, 17%, and 0% of the total occurred in Beam 2, Beam 3, and Beam 4, respectively. From the field measurements, these same percentages were 58%, 27%, 15%, and 0%. A comparison between the field and analytical prediction is shown in Figures 38 and 39. Both the analysis and the field test results showed that applying P-T force on one of the exterior beams has negligible effect on the other exterior beam. In general, both results produced a good agreement; however, it was generally found that the experimental strains were higher than the theoretical strains.

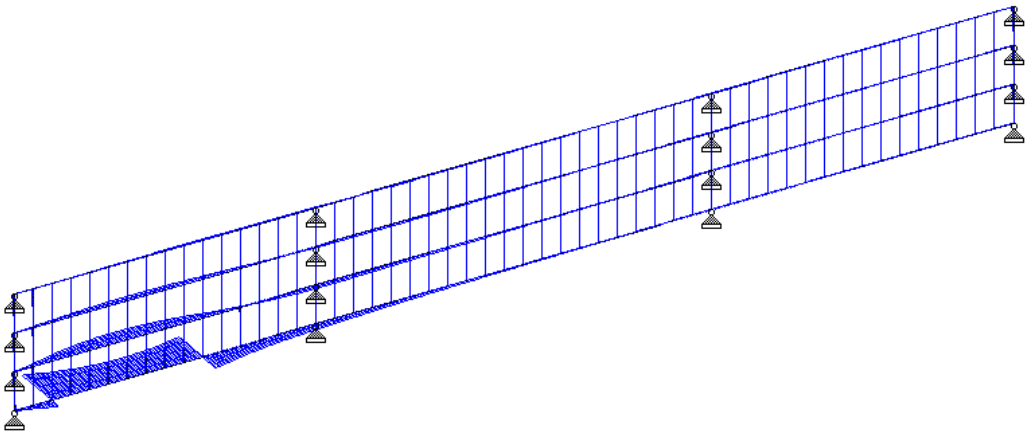

(a) P-T west end span Beam 4

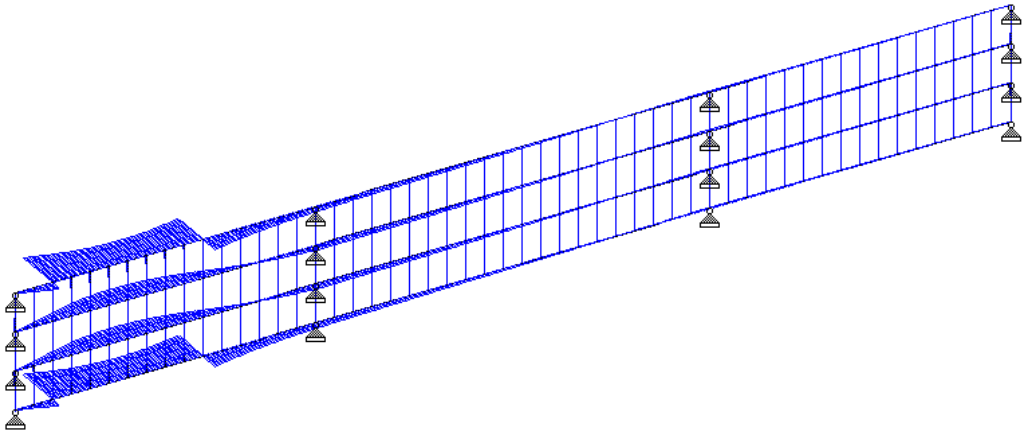

(b) P-T west end span Beam 1

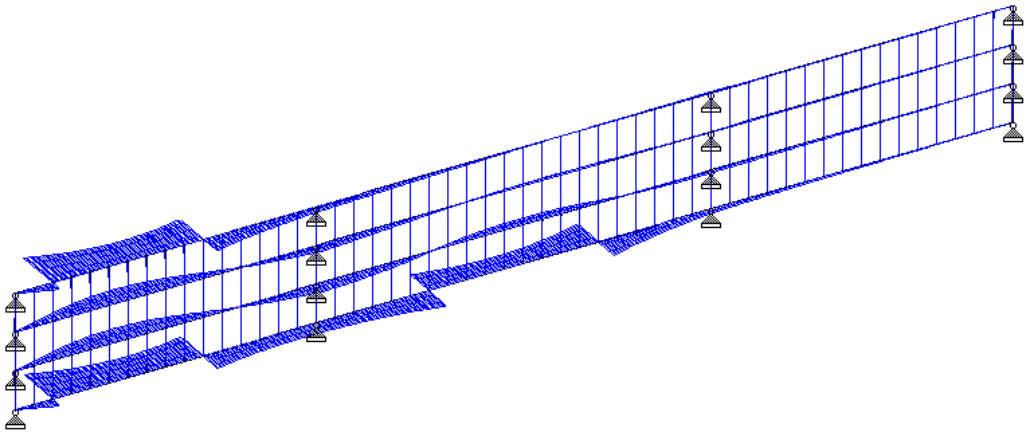

(c) P-T center span Beam 4

Figure 37. Theoretical P-T induced internal moments.

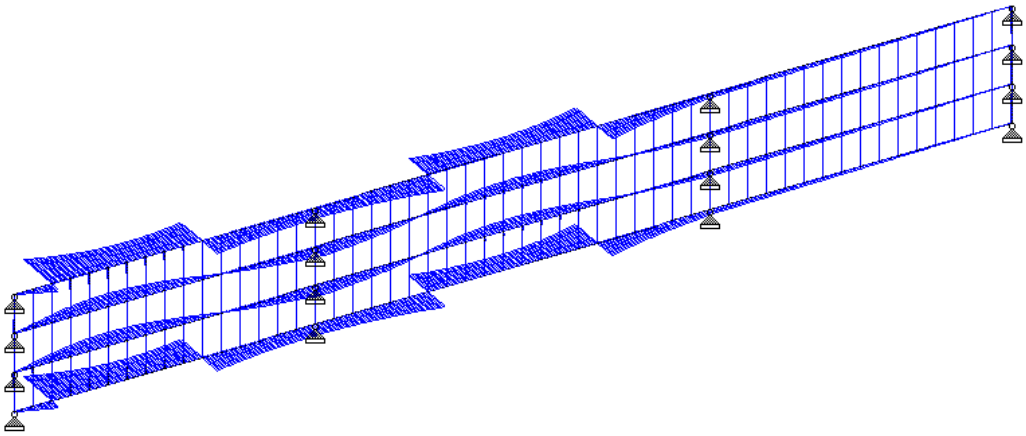

(d) P-T center span Beam 1

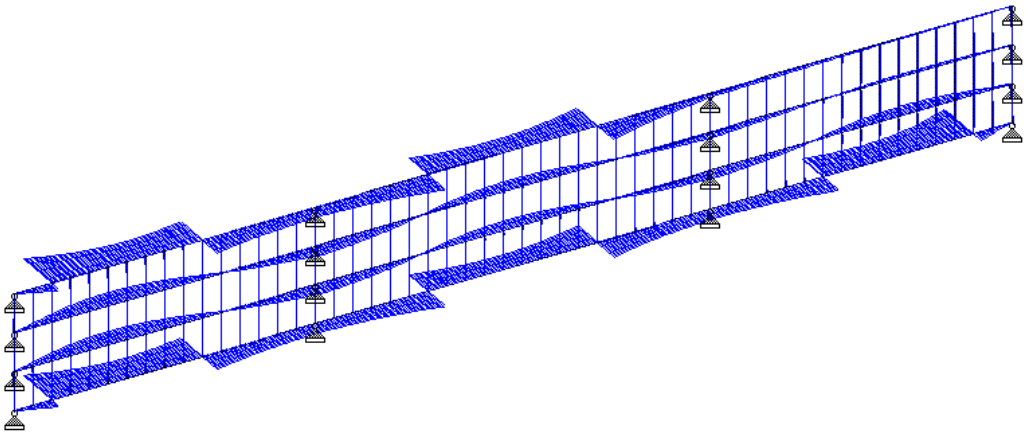

(e) P-T east end span Beam 4

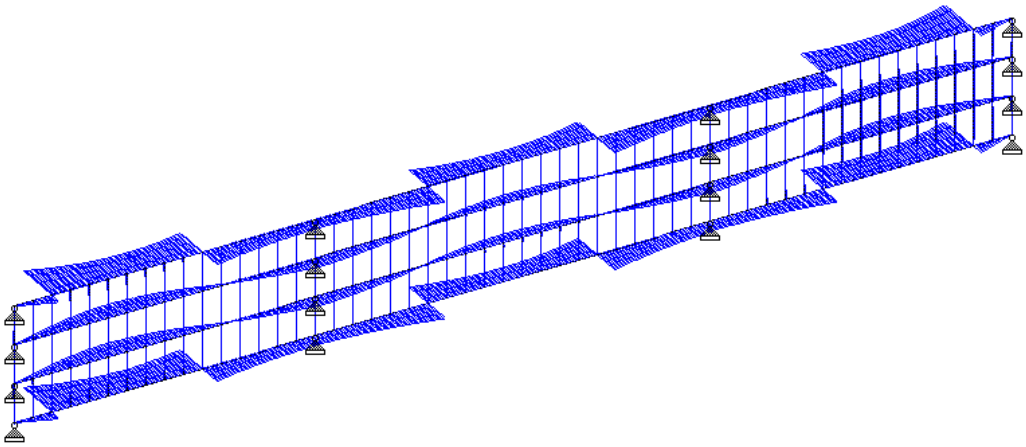

(f) P-T east end span Beam 1

Figure 37. Theoretical P-T induced internal moments (continued).

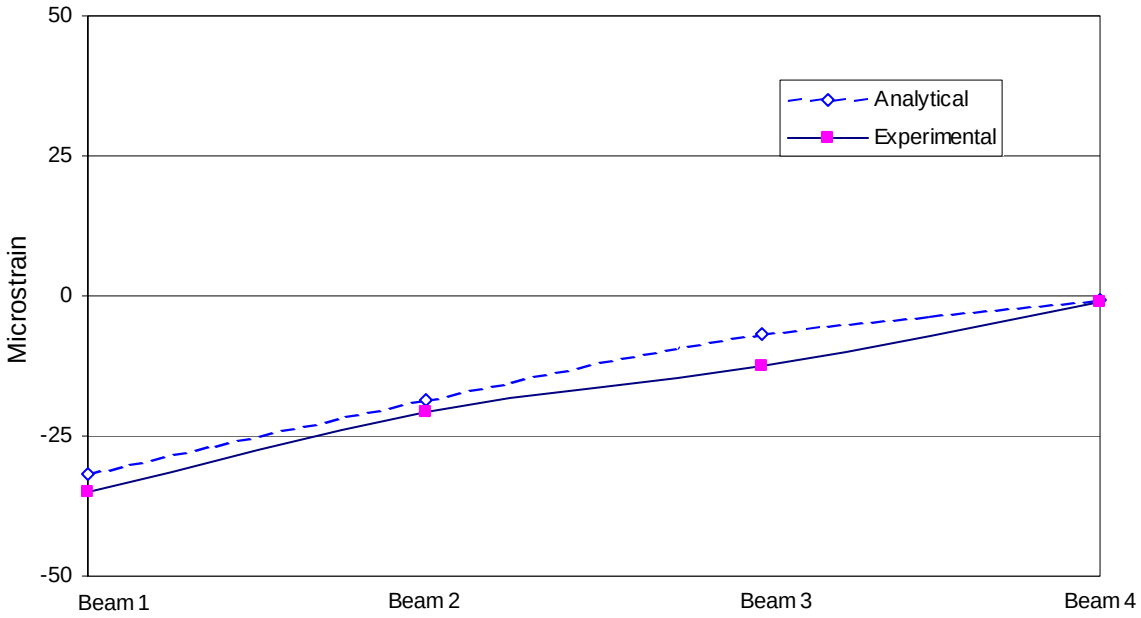

Figure 38. Strains at Section B during P-T west end span, Beam 1.

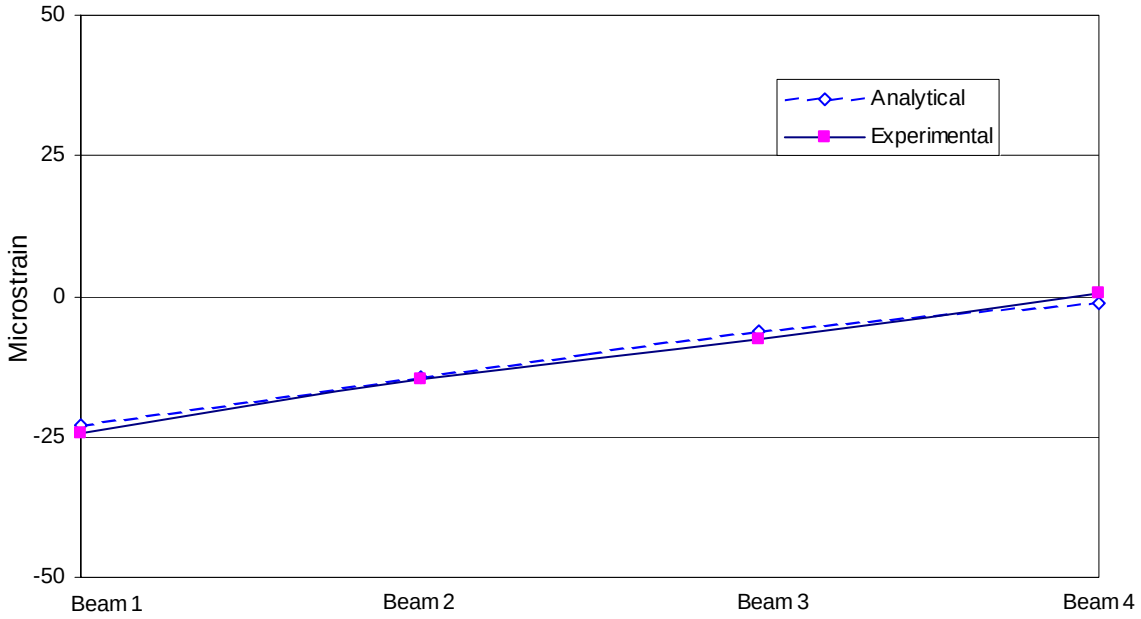

Figure 39. Strains at Section D during P-T center span, Beam 1.

4.2.4.2. INDIVIDUAL BEAM ANALYSIS

To illustrate how the P-T strengthening system improves the live load carrying capacity of the subject bridge, an analysis was performed on both an exterior and interior girder. The moment induced by the P-T force, dead load, and live load at each location of the bridge will be presented first and then combined to illustrate the overall impact of the P-T strengthening system. For this analysis, the live load moment was determined using an HS-20 truck [10] placed so that the maximum positive moment could be generated. Note that the moment diagrams presented in this section are not to scale. Also, from the grillage analysis, the strain induced by the concentric axial force was found to be negligible (i.e., in the range of approximately 0 to 3 microstrain); therefore, a reduction of bottom flange stress due to this axial force component was not included in this analysis.

As was described previously, the lateral distribution factors at the maximum positive moment region were, on average, 58% for the exterior and 42% for the interior beam. Given these distribution factors, the P-T induced moments for the exterior and interior beam at each midspan gage location (Sections B and D) were determined. Figures 40 and 41 show the interior and exterior beam moments induced by the dead load and P-T force, respectively. As can be seen, the P-T force generates moments opposite in sign to those induced by the dead load at both the maximum positive moment region (midspan) and maximum negative moment region (pier). Figure 42 presents a moment diagram with these effects combined. From these, it can be seen that the P-T strengthening system has a positive impact on the maximum positive moment region; a portion of dead load moment are reduced by the P-T induced moment at the maximum positive regions in both end spans (11.5% for the exterior and the 10.3% for interior beam) and in the center span (6.9% for the exterior and 6.0% for the interior beam).

Three point loads were used to represent the HS-20 truck [10]. These individual point loads were placed so that maximum moments could be generated at the maximum positive moment region in each span. The lateral distribution factors for the exterior and the interior girder determined based upon AASHTO standard specification [10] were applied to the live load induced moment. The experimental lateral distribution factors obtained during the application of the P-T force were used in computing the P-T induced moment. An illustration of the HS-20 truck positioned in each span and corresponding live load moment diagrams are shown in Figures 43 and 44.

Given the P-T induced moment ($M_{P\text{-}T}$), dead load moment (M_{DL}) and live load moment (M_{LL}), it is now possible to investigate an overall effect of the P-T strengthening system on the bridge by adding all the moments as if the resulting moment is generated by each individual force acting simultaneously as is illustrated in Figures 45 and 46.

As expected, the exterior girder showed a larger reduction in total moment than the interior girder in both the end and the center spans. In general, the end span showed larger moment reductions than the center span. The P-T strengthening system reduced the total moment by 5.3% on the exterior beam and 4.6% on the interior beam in the end span. Similarly, 3.3% and 2.7% of the total moment were reduced on the exterior and the interior beam in the center span, respectively. Overall, the reduction of these moments indicates the P-T strengthening system was effective in decreasing the total moment by approximately 3% to 5% depending upon the locations, and thereby improving the live load carrying capacity of the bridge at the maximum positive moment region. The reduction in total moment by the P-T strengthening system is summarized in Table 9.

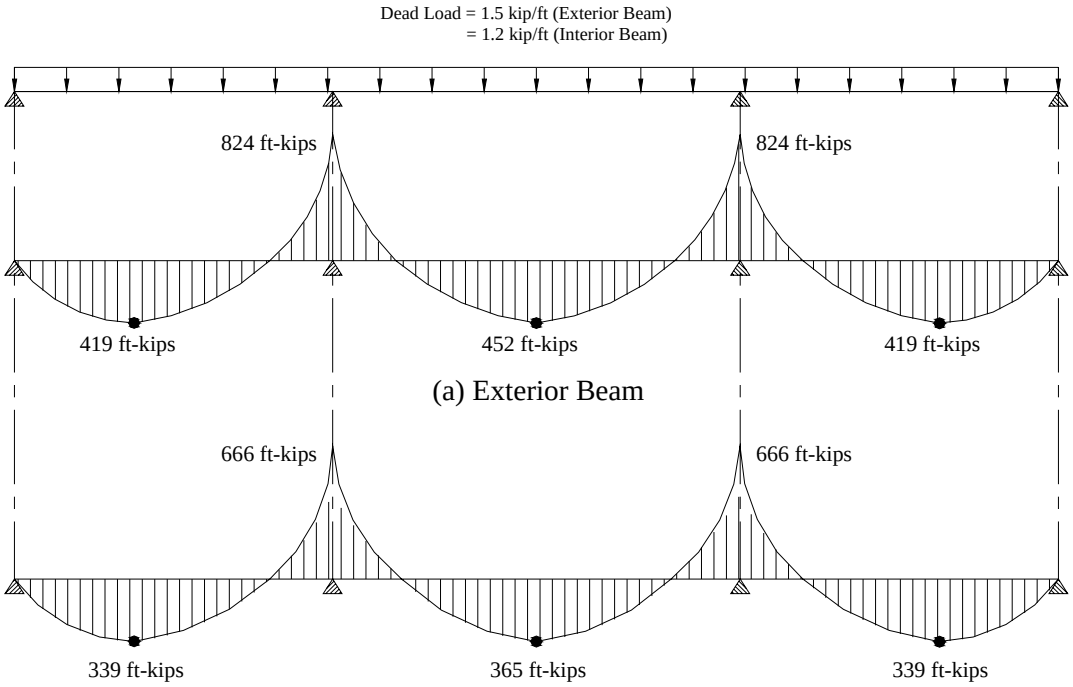

Figure 40. Dead load induced moments.

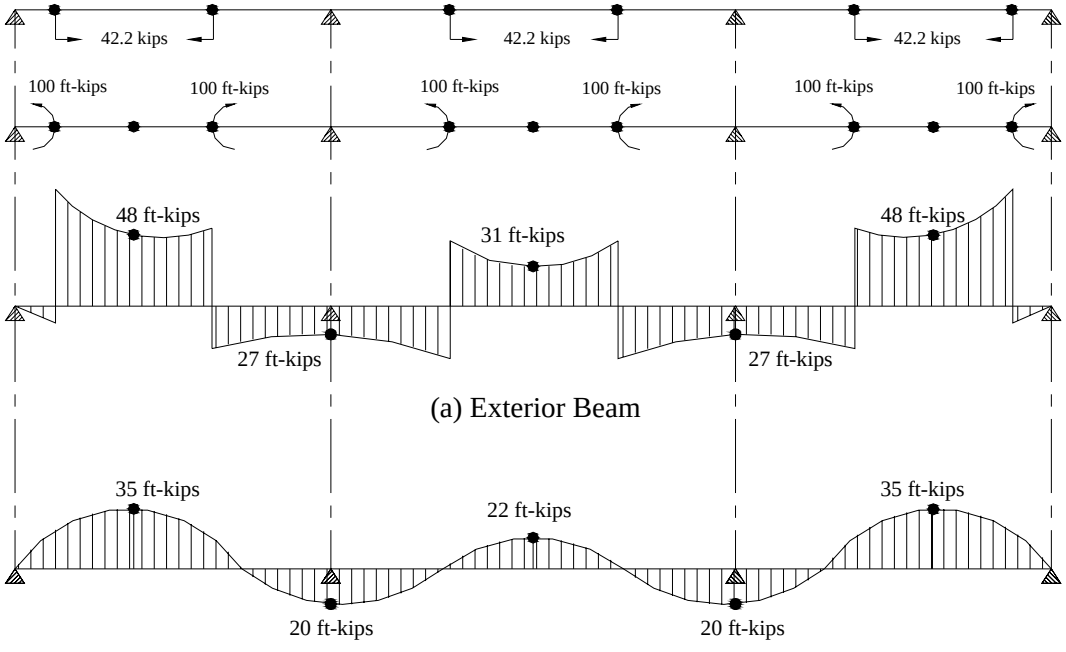

Figure 41. P-T induced moments.

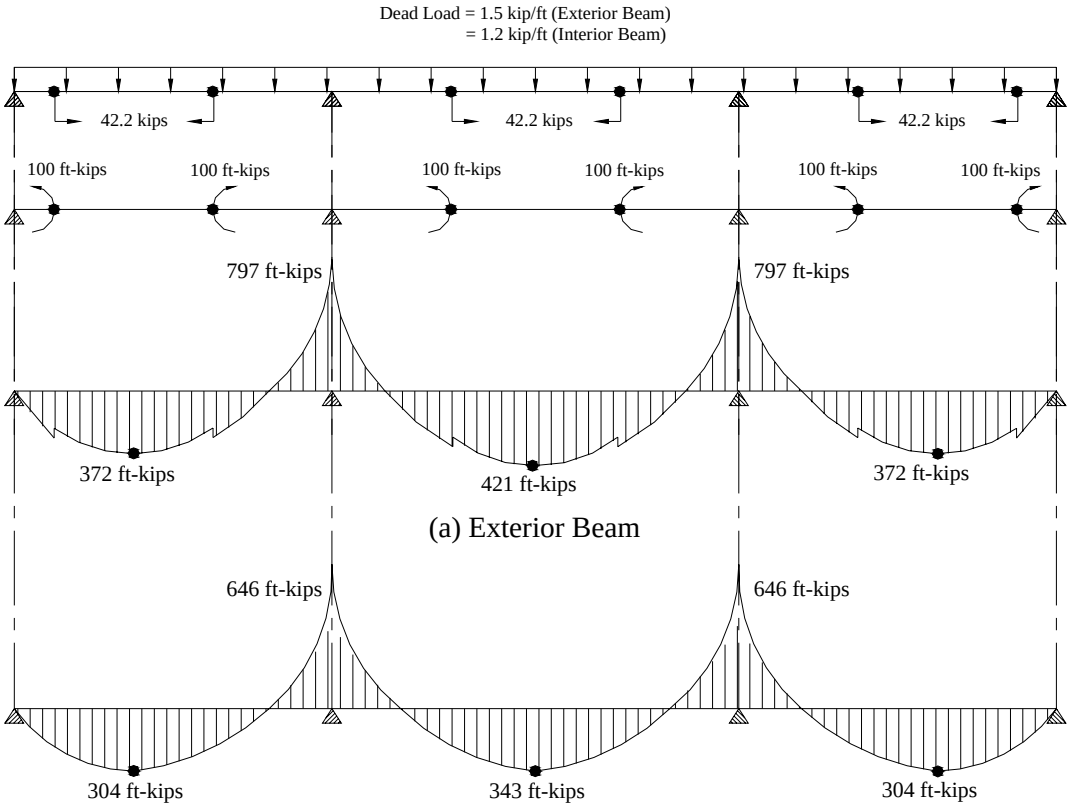

Figure 42. Dead load plus P-T induced moments.

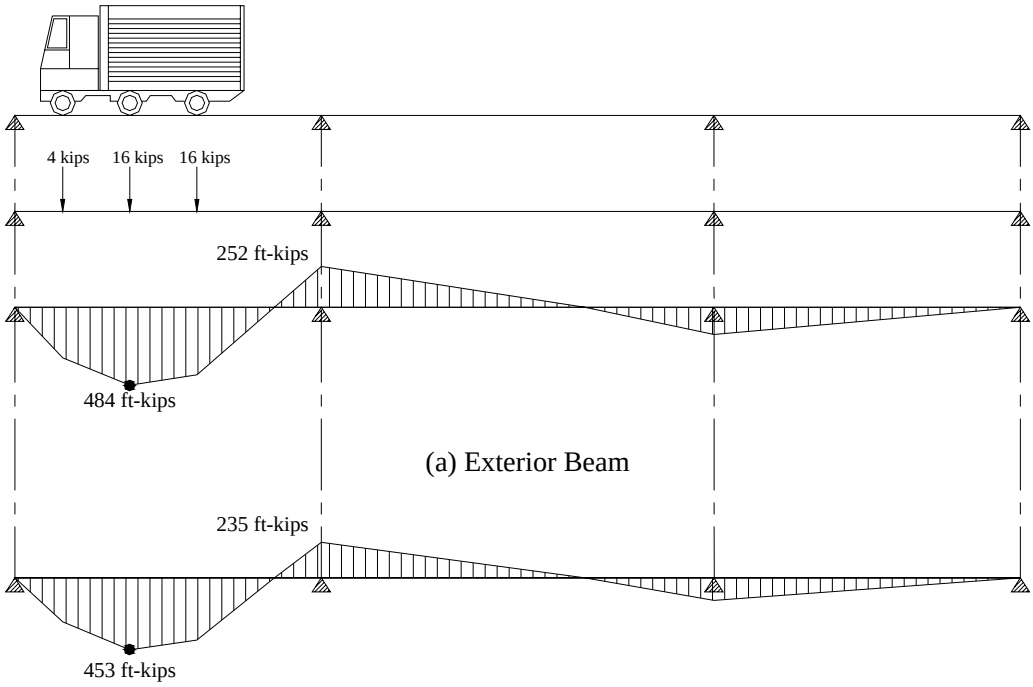

Figure 43. Live load induced moments in the west end span.

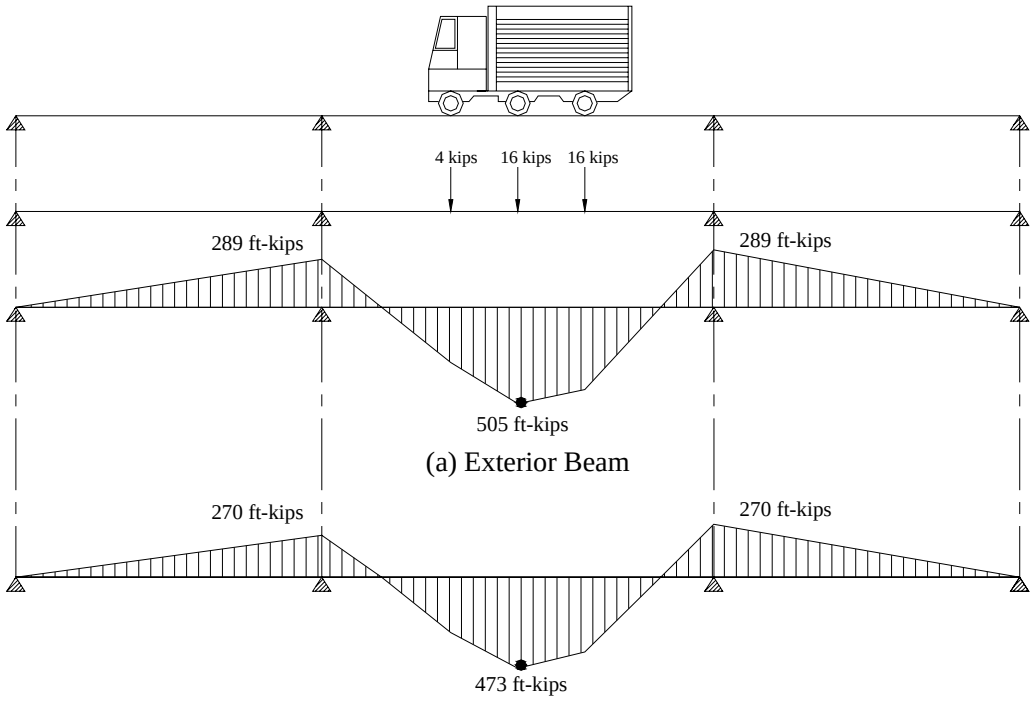

Figure 44. Live load induced moments in the center span.

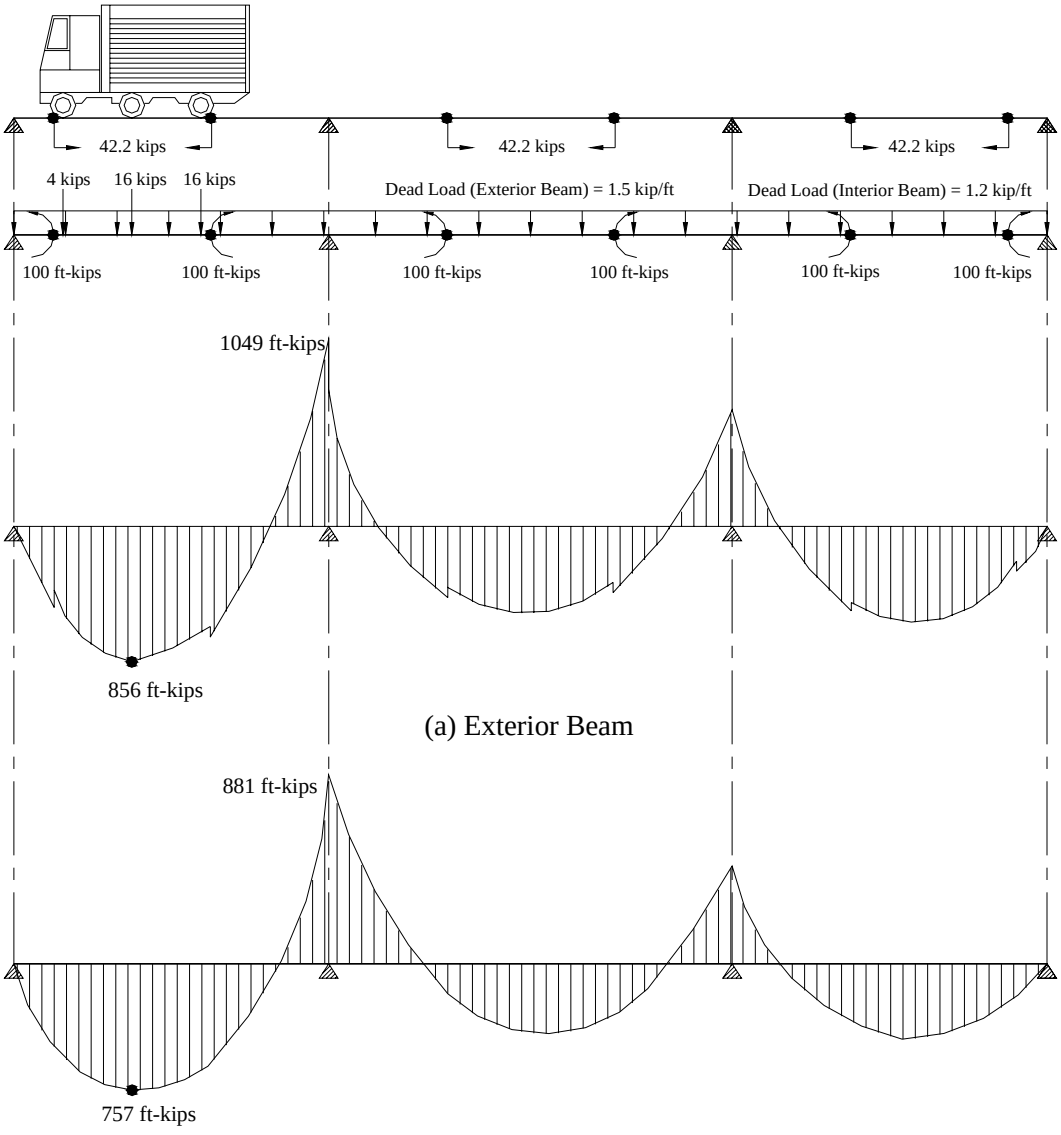

Figure 45. Effect of P-T on maximum moments in the west end span.

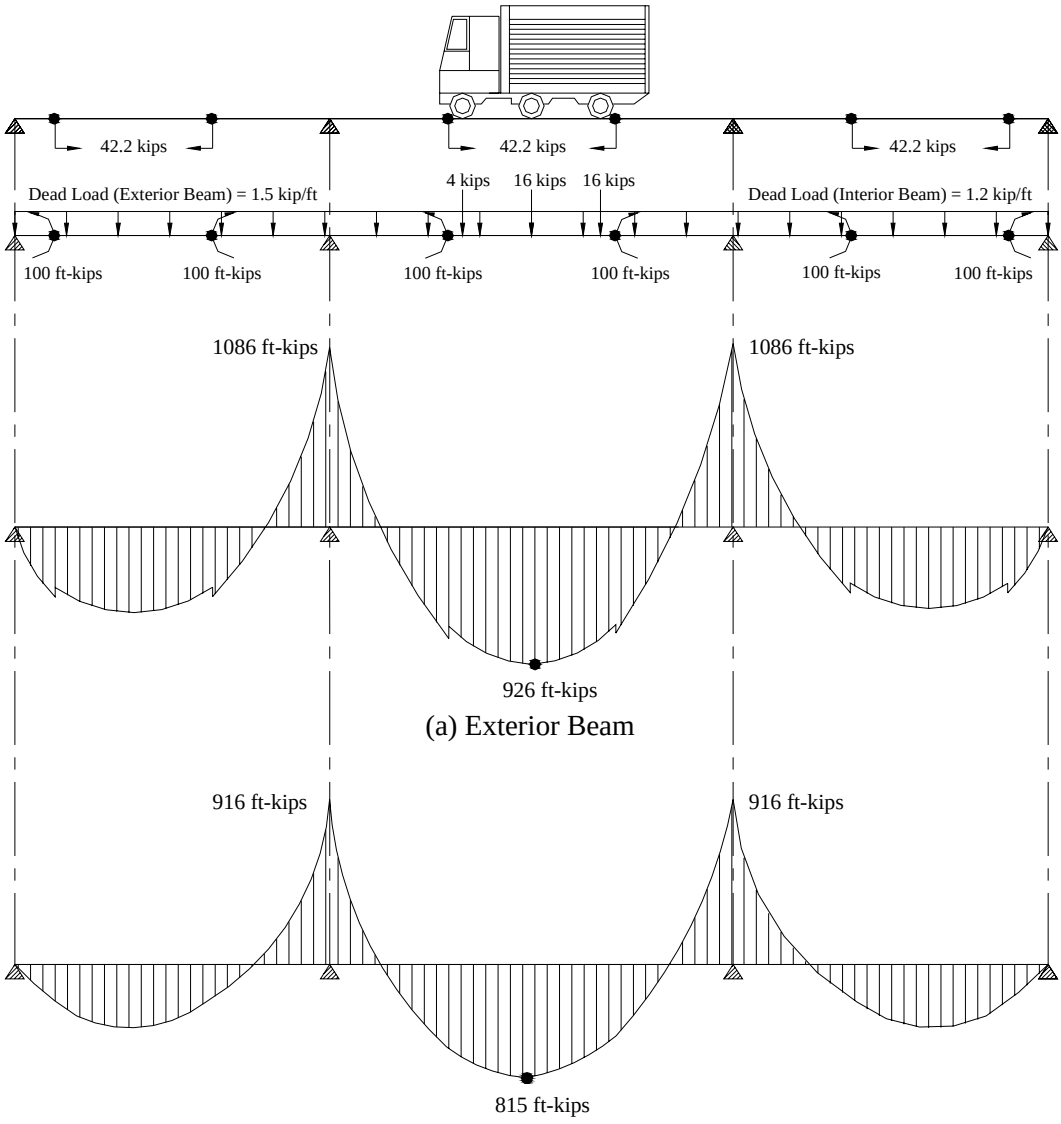

Figure 46. Effect of P-T on maximum moments in the center span.

Table 9. Reduction in total moment by the P-T strengthening system.

	Section B		Section D	
	Exterior	**Interior**	**Exterior**	**Interior**
$M_{DL} + M_{LL}$ (ft-kips)	904	792	957	838
$M_{P-T} + M_{DL} + M_{LL}$ (ft-kips)	856	757	926	815
Reduction in moment, %	5.3	4.6	3.3	2.7

4.2.5. Change in Post-tensioning Force over Time

As was previously mentioned in Chapter 3, the P-T force was removed from the bridge after two years of service so that any losses could be determined. Recall that the forces were removed following the sequence shown in Figure 21. Figure 47 illustrates the force levels present in each bar. In comparison with the forces that were originally applied, it was found that the largest loss (3.7 kips – 7.8%) occurred on Beam 1 in the center span while the average loss was 2.6 kips (5.4%). Although some loss of P-T force occurred in most bars, it should be noted that these losses were accounted for during the design phase (see section 2.2.1).

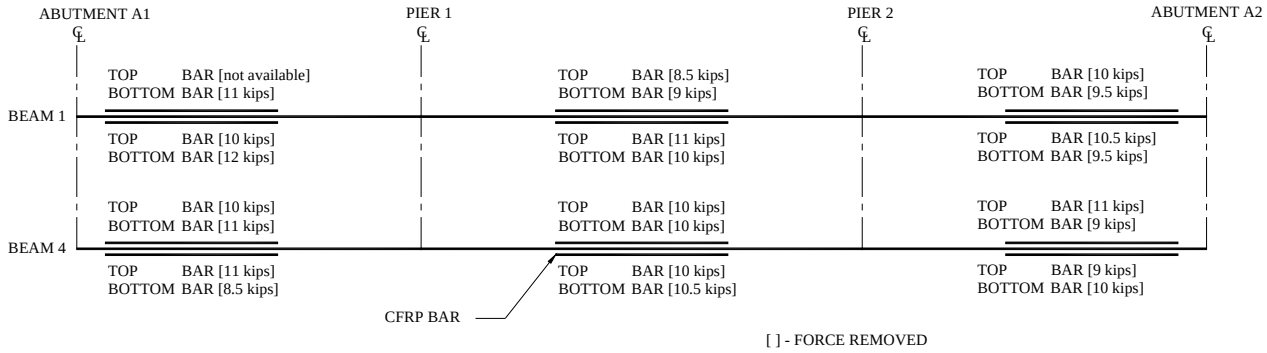

Figure 47. P-T forces removed from each bar.

5. SUMMARY AND CONCLUSIONS

5.1. Summary

The bridge selected for strengthening was a three-span, continuous steel stringer bridge in Guthrie County, Iowa, on state highway IA 141 approximately 1.6 miles west of Bayard, Iowa. The goal of this project was to design and install CFRP post-tensioning bars on the exterior steel girders and to monitor and document the performance and long-term impact of the strengthening system. The research program consisted of several tasks with the main emphasis being the design and installation of the strengthening system and associated field testing.

Before the P-T system was installed, a diagnostic load test was conducted on the subject bridge to establish a baseline behavior of the unstrengthened bridge. During installation of the P-T hardware and stressing of the system, both the bridge and P-T system were monitored. The installation of the hardware was followed by a diagnostic load test to assess the immediate effectiveness of the P-T strengthening system. Additional load tests were performed over a two-year period to identify changes in the strengthening system with time. After the last load test (after two years of service) was completed, the P-T force was removed from the bridge (and subsequently re-applied) to investigate any losses that may have occurred. Laboratory testing of several typical CFRP bar specimens was also conducted to more thoroughly understand their behavior.

5.2. Conclusions

5.2.1. Laboratory Test

CFRP bars were tested in the laboratory to better understand their characteristics and to assess the feasibility of the CFRP bars as a strengthening material. The following conclusions were generated based upon the test results:

- From visual observation and experimental results from the laboratory 24-hour, constant load test, the slippage between the bar and grip connection was very small (0.0011 in.). Therefore, no conclusions can be drawn from the laboratory test as to the cause of the slip observed in the field.
- During the ultimate strength test, each specimen experienced several localized fiber failures before the specimen failed, and significant strength decrease occurred. However, the tensile strength of all tested specimens exceeded the nominal force (12 kips) applied in the field.

5.2.2. Installation of CFRP Post-tensioning System

- The installation of the P-T system required no special equipment or training other than access equipment, an acetylene torch to remove a portion of several diaphragms, and a hydraulic jack for the application of the P-T force to the CFRP bars. A three-person crew was able to install the system in just over one day.

5.2.3. Field Test

Based upon the monitoring and testing conducted in the field, several conclusions were drawn and summarized as follows:

- The addition of the P-T strengthening system had a negligible impact on changing the stiffness of the bridge. This indicates that the live load distribution characteristics are virtually the same before and after the installation of the P-T strengthening system.
- The P-T system generates strain opposite to those produced by dead and live loads and thereby improves the overall live load carrying capacity of the bridge.
- Based upon an analysis performed using the HS-20 truck, it was found that the P-T strengthening system reduced dead and live load induced moments by approximately 3% to 5%, thus allowing the bridge to carry additional live load.
- An average loss of 2.6 kips of P-T force (per location) occurred over two years of service; therefore, long-term monitoring on the P-T strengthening system maybe needed for further assessment.
- The use of the P-T CFRP bars to strengthen the structurally deficient bridge described in this project was proved to be a viable, effective, and practical solution. However, the CFRP P-T bars used in this project may not be applicable where larger overstresses need to be reduced. In such a case, a bar with increased capacity may be needed.

6. REFERENCES

1. Klaiber, F. W., K. F. Dunker, and W. W. Sanders, Jr. *Feasibility Study of Strengthening Existing Single Span Steel Beam Concrete Deck Bridges*. Iowa DOT project HR-214 final report. Ames, IA: Department of Civil Engineering, Iowa State University, 1981.

2. Dunker, K. F., D. J. Dedic, and W. W. Sanders, Jr. *Strengthening of Existing Single-Span Steel-Beam and Concrete Deck Bridges*. Iowa DOT project HR-238 part I final report. Ames, IA: Engineering Research Institute, Iowa State University, 1983.

3. Dunker, K. F., F. W. Klaiber, B. L. Beck and W. W. Sanders, Jr. *Strengthening of Existing Single-Span Steel-Beam and Concrete Deck Bridges*. Iowa DOT project HR-238 part II final report. Ames, IA: Engineering Research Institute, Iowa State University, 1985.

4. Dunker, K. F., F. W. Klaiber, and W. W. Sanders, Jr. *Design Manual for Strengthening of Continuous Span Composite Bridges*. Iowa DOT project HR-238 part III final report. Ames, IA: Engineering Research Institute, Iowa State University, 1985.

5. Dunker, K. F., F. W. Klaiber, F. K. Daoud, W. E. Wiley and W. W. Sanders, Jr. *Strengthening of Existing Continuous Composite Bridges*. Iowa DOT project HR-287 final report. Ames, IA: Engineering Research Institute, Iowa State University, 1987.

6. Klaiber, F. W., F. S. Fanous, T. J. Wipf and H. El-Arabaty. *Design Manual for Strengthening of Continuous Span Composite Bridges*. Iowa DOT project HR-333 final report. Ames, IA: Engineering Research Institute, Iowa State University, 1993.

7. Jones R. F. *Guide to Short Fiber Reinforced Plastics*. New York: Chernow Editorial Services, 1998.

8. Burgoyne J. C. *Advanced Composites in Civil Engineering in Europe*. Cambridge: University of Cambridge, 1999.

9. Tang, B., and W. Podolny. “A Successful Beginning for Fiber Reinforced Polymer (FRP) Composite Materials in Bridge Applications,” in *FHWA Proceedings*, Orlando, FL, December 1998.

10. American Association of State Highway and Transportation Officials. *Standard Specifications for Highway Bridges*. 16th ed. Washington, DC: American Association of State Highway and Transportation Officials, 1996.

APPENDIX: POST-TENSIONING EVENTS

Table A.1. P-T west end span

Event	Beam Number	Beam	Bar	Load (kips)
1	4	Exterior	Bottom	0
2	4	Exterior	Bottom	6
3	4	Exterior	Top	0
4	4	Exterior	Top	6
5	4	Interior	Bottom	0
6	4	Interior	Bottom	6
7	4	Interior	Top	0
8	4	Interior	Top	6
9	4	Interior	Top	12
10	4	Interior	Bottom	6
11	4	Interior	Bottom	12
12	4	Exterior	Bottom	6
13	4	Exterior	Bottom	12
14	4	Exterior	Top	6
15	4	Exterior	Top	12
16	4		Beam 4 completed	
17	1	Interior	Bottom	0
18	1	Interior	Bottom	6
19	1	Interior	Top	0
20	1	Interior	Top	6
21	1	Exterior	Bottom	0
22	1	Exterior	Bottom	6
23	1	Exterior	Top	0
24	1	Exterior	Top	6
25	1	Exterior	Top	12
26	1	Exterior	Bottom	6
27	1	Exterior	Bottom	12
28	1	Interior	Bottom	6
29	1	Interior	Bottom	12
30	1	Interior	Top	6
31	1	Interior	Top	12
32	1		Beam 1 completed	

Table A.2. P-T center span

Event	Beam Number	Beam	Bar	Load (kips)
33	4	Exterior	Bottom	0
34	4	Exterior	Bottom	6
35	4	Exterior	Top	0
36	4	Exterior	Top	6
37	4	Interior	Bottom	0
38	4	Interior	Bottom	6
39	4	Interior	Top	0
40	4	Interior	Top	6
41	4	Interior	Top	12
42	4	Interior	Bottom	6
43	4	Interior	Bottom	12
44	4	Exterior	Bottom	6
45	4	Exterior	Bottom	12
46	4	Exterior	Top	6
47	4	Exterior	Top	12
48	4		Beam 4 completed	
49	1	Interior	Bottom	0
50	1	Interior	Bottom	6
51	1	Interior	Top	0
52	1	Interior	Top	6
53	1	Exterior	Bottom	0
54	1	Exterior	Bottom	6
55	1	Exterior	Top	0
56	1	Exterior	Top	6
57	1	Exterior	Top	12
58	1	Exterior	Bottom	6
59	1	Exterior	Bottom	12
60	1	Interior	Bottom	6
61	1	Interior	Bottom	12
62	1	Interior	Top	6
63	1	Interior	Top	12
64	1		Beam 1 completed	

Table A.3. P-T east end span

Event	Beam Number	Beam	Bar	Load (kips)
65	4	Exterior	Bottom	0
66	4	Exterior	Bottom	6
67	4	Exterior	Top	0
68	4	Exterior	Top	6
69	4	Interior	Bottom	0
70	4	Interior	Bottom	6
71	4	Interior	Top	0
72	4	Interior	Top	6
73	4	Interior	Top	12
74	4	Interior	Bottom	6
75	4	Interior	Bottom	12
76	4	Exterior	Bottom	6
77	4	Exterior	Bottom	12
78	4	Exterior	Top	6
79	4	Exterior	Top	12
80	4		Beam 4 completed	
81	1	Interior	Bottom	0
82	1	Interior	Bottom	6
83	1	Interior	Top	0
84	1	Interior	Top	6
85	1	Exterior	Bottom	0
86	1	Exterior	Bottom	6
87	1	Exterior	Top	0
88	1	Exterior	Top	6
89	1	Exterior	Top	12
90	1	Exterior	Bottom	6
91	1	Exterior	Bottom	12
92	1	Interior	Bottom	6
93	1	Interior	Bottom	12
94	1	Interior	Top	6
95	1	Interior	Top	12
96	1		Beam 1 completed	